Okura Wēiti Sediment Transport Modelling

Numerical Modelling Report

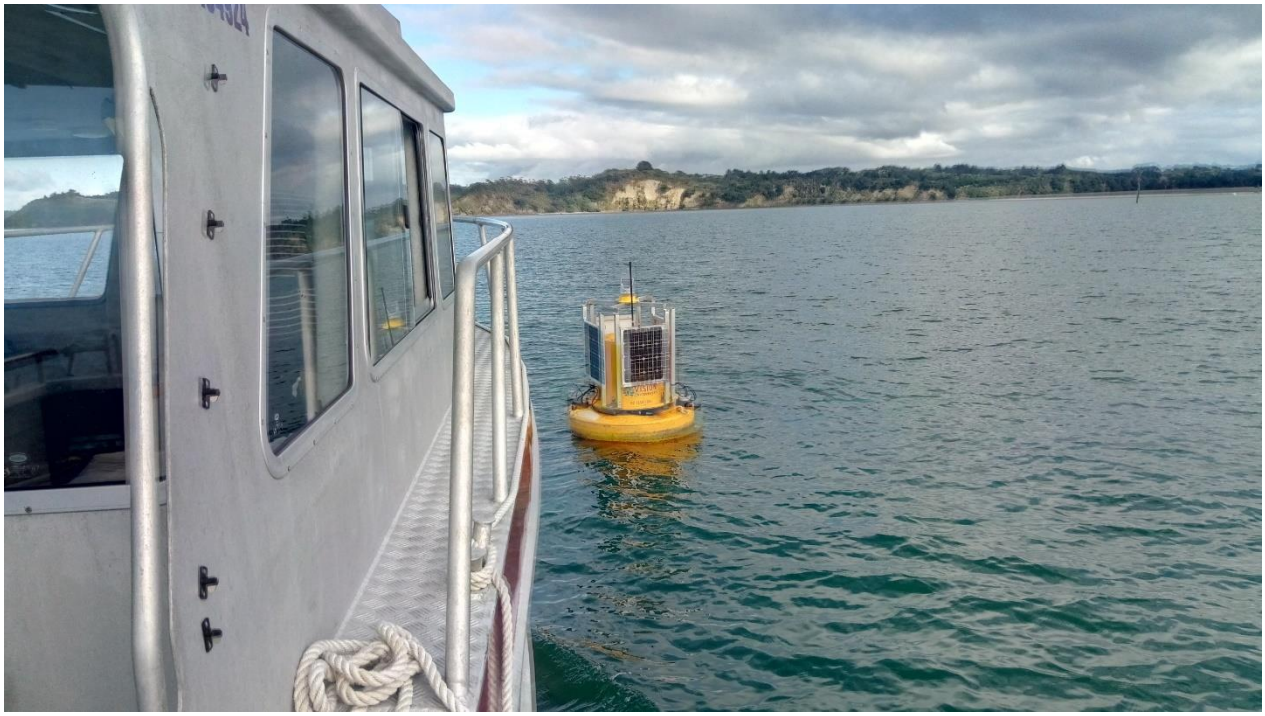

Auckland Council

Report 44801163/01

February 2019

Okura Wēiti Sediment Transport Modelling

Numerical Modelling Report

Prepared for Auckland Council

Represented by Tom Porter

Instrument buoy, Vision Environment

Project manager	John Oldman

Project number	44801163
Approval date	18th February 2019
Revision	Final

DHI Water and Environment Ltd• B:HIVE, Smales Farm• Takapuna 0622 Auckland• New Zealand•
Telephone: +64 9 912 9638 • Telefax: • info.nz@dhigroup.com• www.dhigroup.com

CONTENTS

1 Introduction

There is potential for future development within the catchments which surround the Weiti and Okura estuaries, to have an accumulative effect on the marine receiving environment, due to increased sediment and contaminant loads during construction. The ecology value of the area is recognised by the creation of the Long Bay - Okura Marine Reserve and its designation as a Significant Ecological Area Marine 1 in the Auckland Unitary Plan.

Previous studies have focused on development within the Okura catchment and its potential ecological effects within Okura estuary itself. There has been limited work to date to assess the potential for combined effects of future developments within the Okura, Weiti and Weiti Forest Block catchments.

In addition, previous sediment transport models have not included a wave model and have been used to model schematic events (i.e. constant freshwater flow and suspended sediment concentrations at catchment outlets and fixed tide range and wind speeds and directions.

This report provides details of site-specific data that has been collected from March to July 2018 within Karepiro Bay and the Long Bay-Okura Marine Reserve.

The field data includes a number of days when more than 30 mm of rain fell, a broad range of wind conditions (included an April event where recorded winds were close to the highest on record) and a wave event in June (associated with a subtropical low) when a significant wave height of 1.9 m was recorded.

The field data that has been collected, indicates during periods of higher rainfall, waves of more than 0.5 m significant wave height can be expected within Karepiro Bay. During such events, turbidity data increases by an order of magnitude compared to periods of no waves. During some of these wave events, very high deposition rates are observed while for other wave events, net erosion is observed.

This data will be used to validate an improved hydrodynamic, wave and sediment transport model of the Okura-Weiti marine receiving environment. This will involve the following:

1. The model predictions of currents, water levels and waves will be compared to observations for a range of tide and wind conditions.

2. Salinity data will be used to ensure that the model adequately simulates the dispersion and movement of freshwater in the Long Bay-Okura marine receiving environment.

3. Predicted suspended sediment concentration and bed level change will be compared to the observed data.

The calibrated model will then be used to simulate a range of potential catchment derived sediment and contaminant loads, so that the potential for ecologically significant impacts within different sub-environments within the Okura/Weiti/Karepiro Bay system can be quantified.

Input data for this phase of the work will be derived from work being carried out by Morphum as part of the development of the Freshwater Management Tool.

2 Methods

This section describes the methodology applied to undertake the sediment transport modelling in the Weiti and Okura estuaries. It details the numerical model modelling strategy, model domain and bathymetry, boundary conditions, atmospheric forcing river discharges and sea bed characteristics.

2.1 Numerical Model

The MIKE 21 & 3 systems were used in this study to simulate the wave, hydrodynamic and sediment transport processes. For this purpose, four modules were coupled on a unique unstructured mesh grid to simulate the numerous interactions between the physics and the morphodynamics. For coastal areas such as estuaries or bays, unstructured mesh grids provide an optimal degree of flexibility in the representation of complex geometries. It allows increasing the computational resources on areas where more precision is required while maintaining an acceptable level of details elsewhere in the domain.

The Hydrodynamic Module (HD) included in MIKE 3 (DHI, 2017a) was used to simulate the three-dimensional (3D) flows, surface elevation, sea temperature and salinity over the domain solving the 3D incompressible Reynolds averaged Navier-Stokes equations subject to the assumptions of Boussinesq and of hydrostatic pressure. The model consists of continuity, momentum, temperature, salinity and density equations and it is closed by a turbulent *k-epsilon* closure scheme.

The Spectral Wave Module (SW) was applied to simulate the generation and propagation of waves from the global scale to the local scale. MIKE 21 SW captures the following physical processes:

- Wave growth by wind action
- Non-linear wave-wave interaction
- Dissipation due to whitecapping, bottom friction and depth-induced wave breaking
- Refraction and shoaling due to depth variations
- Wave-current interactions
- Effect of time-varying water depth

Further details about the SW module are provided in (DHI, 2017b).

The transport of cohesive fine-sand, silt and clay particles is modelled in the present study using the Mud Transport (MT) module (DHI, 2017d). This add-on module to MIKE 3 allows simulating the processes of flocculation, hindered settling and consolidation while calculating the rates of erosion, deposition and resuspension of fine particles under current and wave actions. This tool is particularly well-adapted for areas where the suspended riverine silt particles enter the ocean characterised by increasing water depths, multi-directional waves and currents.

2.2 Modelling Approach

The numerical model has been first calibrated against measurements of water elevations, currents, waves and bed changes in Karepiro Bay between March and July 2018. The main purpose of this process was to determine the capability of the model in capturing the dominant morphological processes.

The second stage of the study was to assess the effect of the river discharges on the local sediment transport in Karepiro Bay. To meet this objective, a range of scenarios characterised by different river flows and sediment-suspended concentrations at the discharge locations was tested. This phase of work will be presented in a separate report which will provide a summary of model outputs for the Current State and future scenarios being considered (Table 2-1).

Table 2-1. Scenario conditions for evaluation of potential impact to Long Bay-Okura Marine Reserve.

Scenario	Weiti Development	Surrounding Land Use	Stormwater management requirements for development areas	Levels of Cu, Zn and TSS
1	Existing Development	Current	Existing Treatment from LSPC	Draft calibrated regional LSPC loads -
2	550 homes	Current	SMAF1/GD01	Draft calibrated Regional LSPC loads -
3	1200 homes	Current	SMAF1/GD01	Draft calibrated Regional LSPC loads -
4	Existing Development	Future growth	SMAF1/GD01	Draft calibrated Regional LSPC loads -
5	550 homes	Future growth	SMAF1/GD01	Draft calibrated Regional LSPC loads
6	1200 homes	Future growth	SMAF1/GD01	Draft calibrated Regional LSPC loads
7	1200 homes	Future growth	SMAF1/GD01	More buildup/wash-off
8	1200 homes	Future growth	SMAF1/GD01	Less buildup/wash-off

2.3 Model Domain and Bathymetry

The model domain covers the entire Hauraki Gulf. The mesh grid used in MIKE 21 SW and MIKE 3 is composed of 14,916 triangular elements relatively coarse in both the northern and the eastern regions of the domain and refined in Karepiro Bay, Okura River and Weiti River (Figure 2-1). A 43 km wide open boundary has been applied between Takatu Point and Port Jackson on the western and eastern sides of the Hauraki Gulf entrance, respectively.

The model bathymetry has been generated combining chart data from C-MAP (DHI, 2017e) and Auckland Council LIDAR data. A classic linear method has been used to interpolate the Chart Datum referenced water depths on the triangular mesh-grid. Details of the model bathymetry within both the Hauraki Gulf and the Karepiro Bay are shown in Figure 2-2.

The water depth varies from 50 m at the open-ocean boundary to 4 m at the entrance to Karepiro Bay. The western margin of the Karepiro Bay is characterised by inter-tidal areas with water depths lower than 2 m. Alternating inter-tidal areas and shallow margin channels compose both the Okura and the Weiti Rivers.

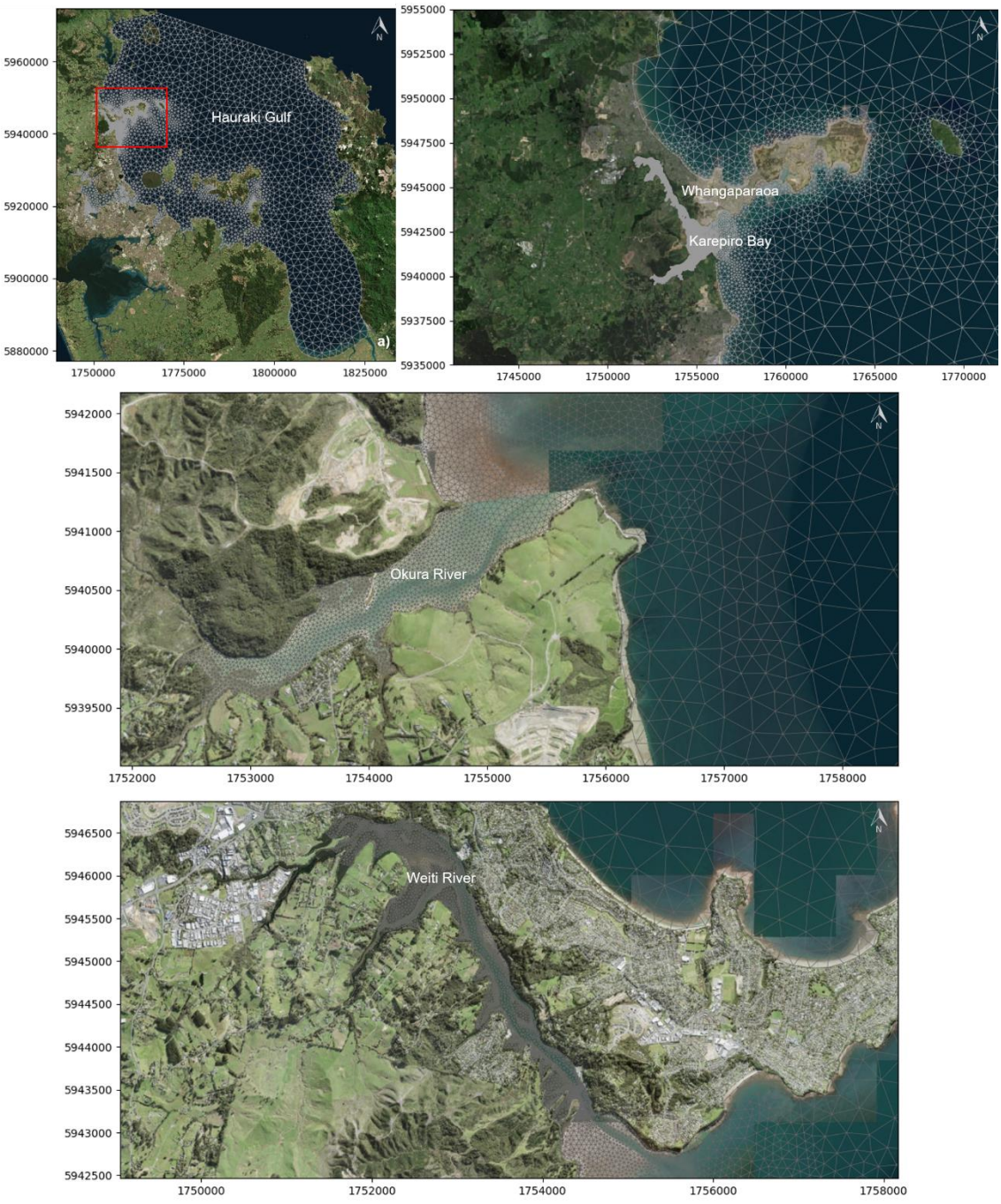

Figure 2-1. Triangular mesh grid used in MIKE 3 to simulate wave, hydrodynamic and sediment transport processes.

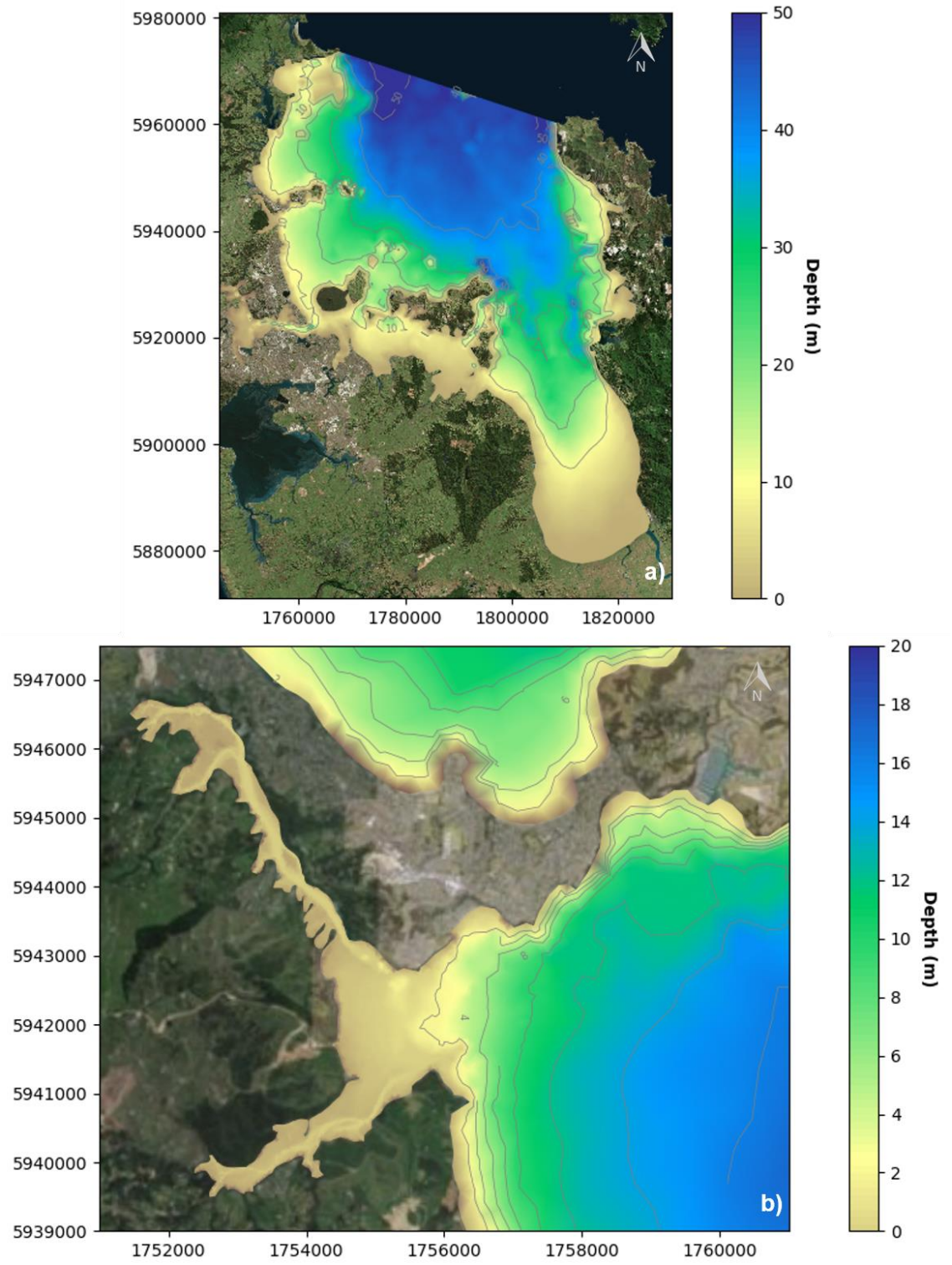

Figure 2-2. Bathymetry (Chart Datum) over the entire model domain (top panel) and within Karepiro Bay (bottom panel) and the Okura and Weiti Rivers.

2.4 Wind Forcing

Regional 6-hourly nowcast surface winds were applied to force both the hydrodynamic and wave models. Validation of these wind data against measurements at Whangaparaoa and Whenuapai has been presented in DHI (2018). Results showed the spatial variability of the wind speed was

well represented in the dataset. However, the model wind direction exhibited a slight shift in the prevailing direction that may influence the local hydrodynamics and waves. The mean, percentile 90 and percentile 99 of the spatial surface wind field calculated between 01/01/2018 and 01/10/2018 are presented in Figure 2-3. Model wind statistics, timeseries and wind rose are provided at Whangaparaoa in Table 2-2, Figure 2-4 and Figure 2-5.

As shown in Figure 2-3, the model wind field exhibits a notable spatial variability over the Hauraki Gulf caused by the complex topography. Such results justify the use of spatial wind field for the numerical modelling rather than space-constant measured wind data. At Whangaparaoa, the mean and maximum wind speed between 01/01/2018 and 01/10/2018 is 5.69 m/s and 17.24 m/s, respectively. Prevailing winds come from the south-western direction while the strongest wind events are dominated by wind directions in the north-eastern quadrant.

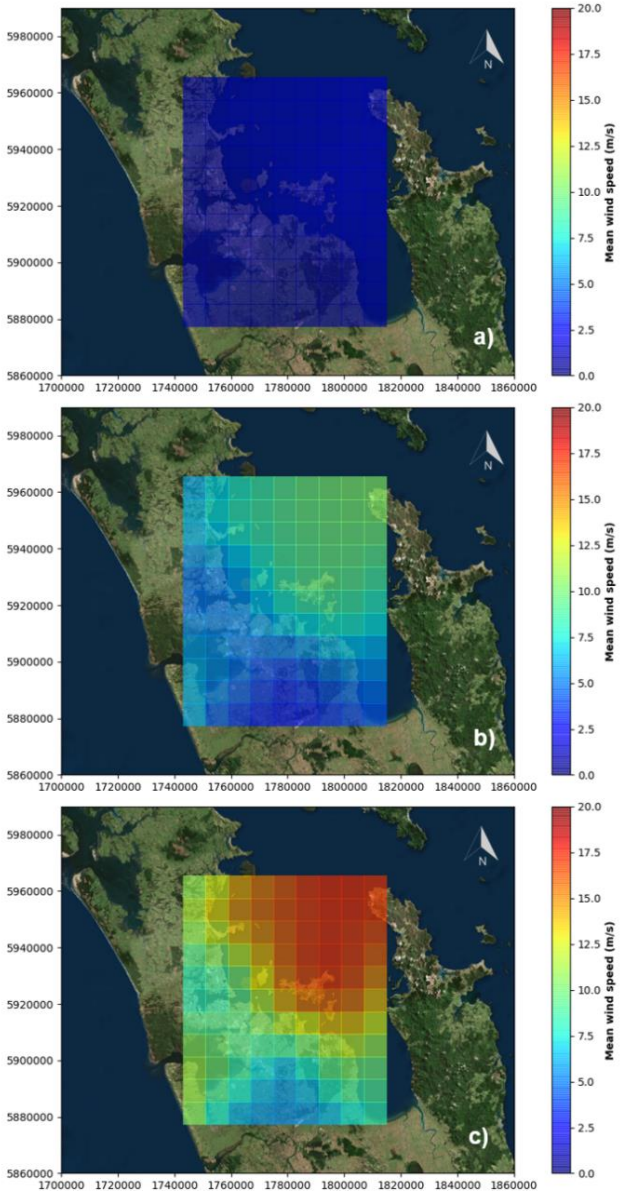

Figure 2-3 Map showing the mean, percentile 90 and percentile 99 of the wind speed field extracted from the nowcast dataset between January and October 2018.

Table 2-2 Wind statistics at Whangaparaoa between January and October 2018.

Wind speed statistics	
(m/s)	
Mean	5.69
Maximum	17.48
P25	3.51
P50	5.22
P75	7.42
P90	9.86
P95	11.14
P99	13.64

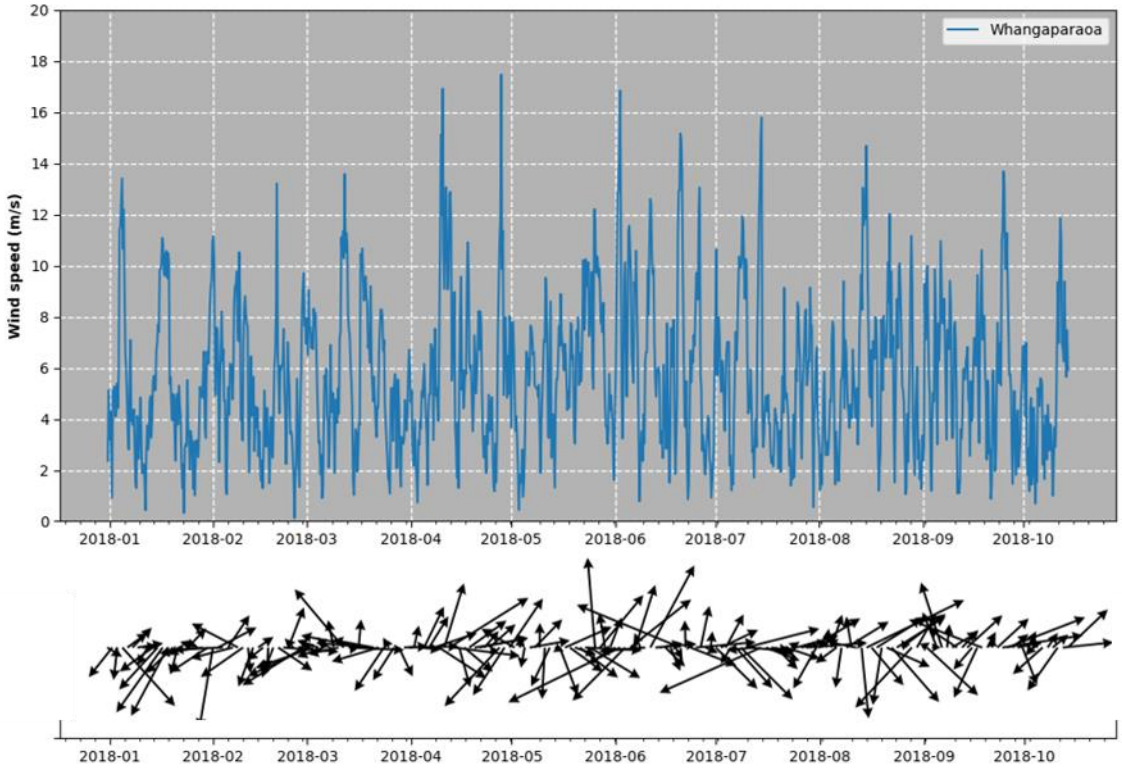

Figure 2-4 Wind speed and direction (“going to”) extracted from the nowcast dataset at Whangaparaoa between January and October 2018.

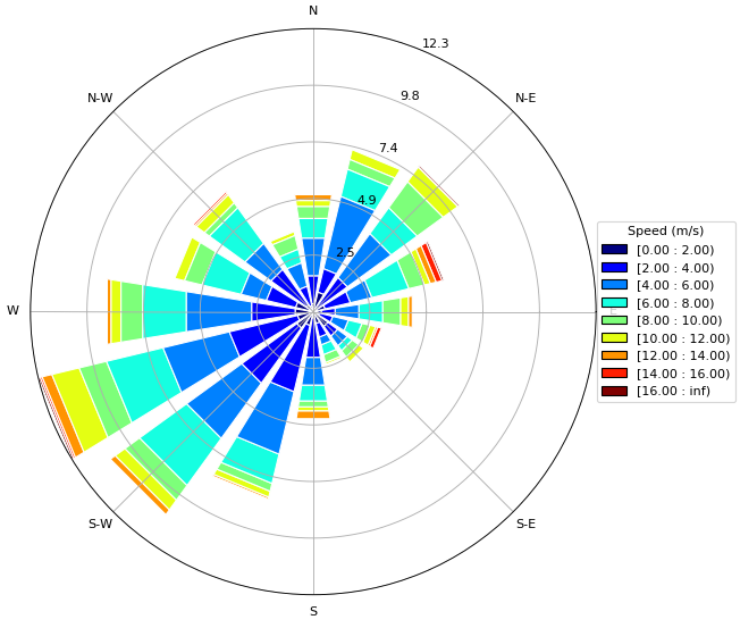

Figure 2-5 Wind rose produced from the nowcast dataset at Whangaparaoa between January and October 2018.

2.5 Boundary Conditions

Open boundary conditions for both the hydrodynamic and the spectral wave models are defined between Takatu Point and Port Jackson (Figure 2-6) at the Hauraki Gulf entrance.

As described in Greig (1990), the Hauraki Gulf is not influenced by consistent, largescale patterns of flow. The net southward flow occurring through the Jellicoe Channel to the North of the Hauraki Gulf is typically deflected toward the Colville Channel without appreciably penetrating the inner gulf. In this context, it is considered that the hydrodynamics within the Hauraki Gulf is dominated by tidal and locally wind-induced currents. For this reason, the hydrodynamic model has been forced at the open boundary using timeseries of tidal water elevation predicted at Port Jackson. The timeseries of water elevation in Figure 2-7 exhibits variations between -1.42 m and 1.44 m, with the Mean Sea Level (MSL) estimated to 1.48 m.

Regarding the wave boundary conditions, the Hauraki Gulf spectral wave model was nested into the New Zealand (NZ) spectral wave model produced by DHI providing hourly two-dimensional (2D) wave spectra at the gulf entrance (Figure 2-8). The timeseries of the model significant wave height and wave rose extracted at the centre of the open boundary from the NZ wave model between 01/01/2018 and 15/09/2018 are shown in Figure 2-9 and Figure 2-10. Although the wave climate within the Hauraki Gulf is dominated by short period sea-waves generated by local wind action, including incoming swells through the narrow gulf entrance improved somewhat the performance of the wave model. Results of the model validation are provided in Section 3.1.

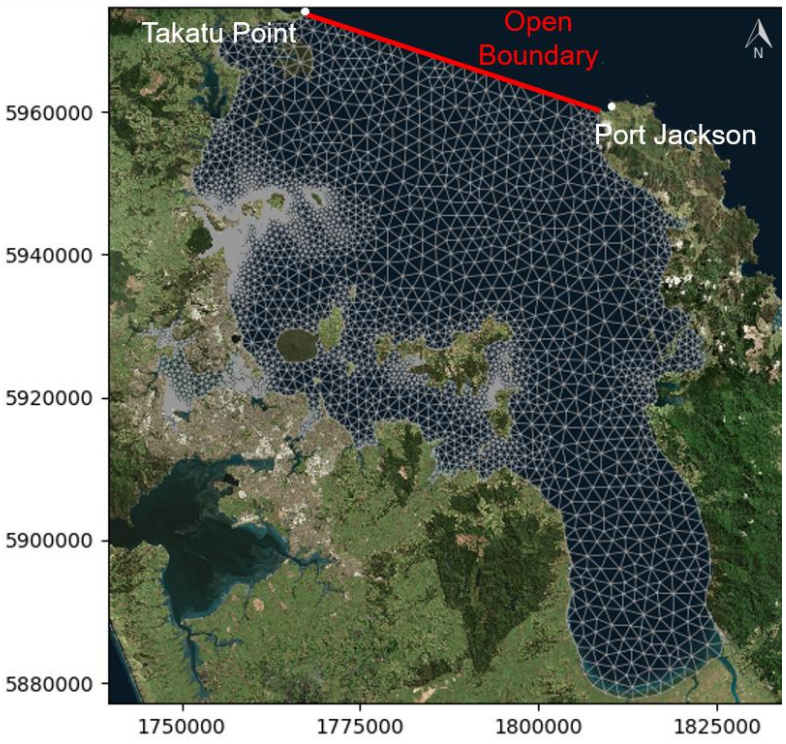

Figure 2-6 Mesh grid including the location of the open boundary forced by tidal water elevations in the hydrodynamic model. The white dot indicates the location of Port Jackson where tidal water elevations have been predicted.

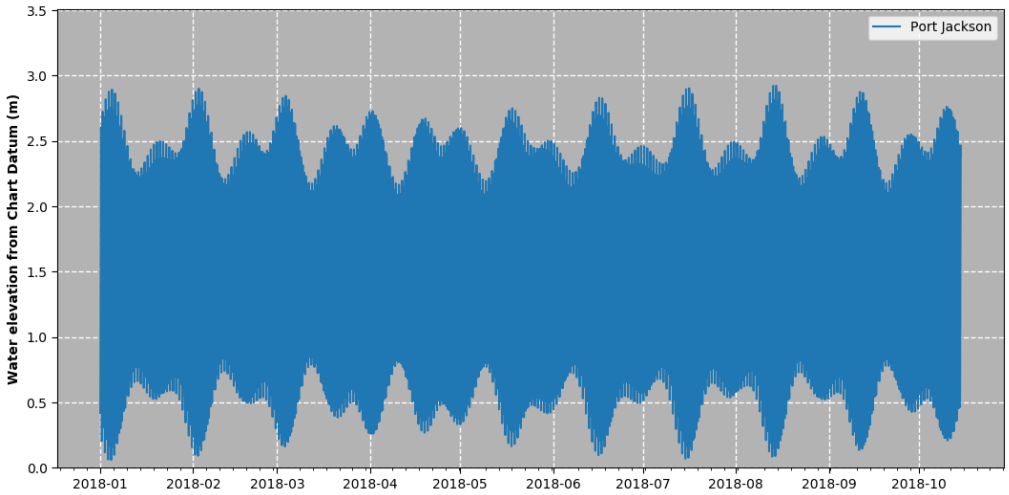

Figure 2-7 Water elevation predicted at Port Jackson between January and October 2018.

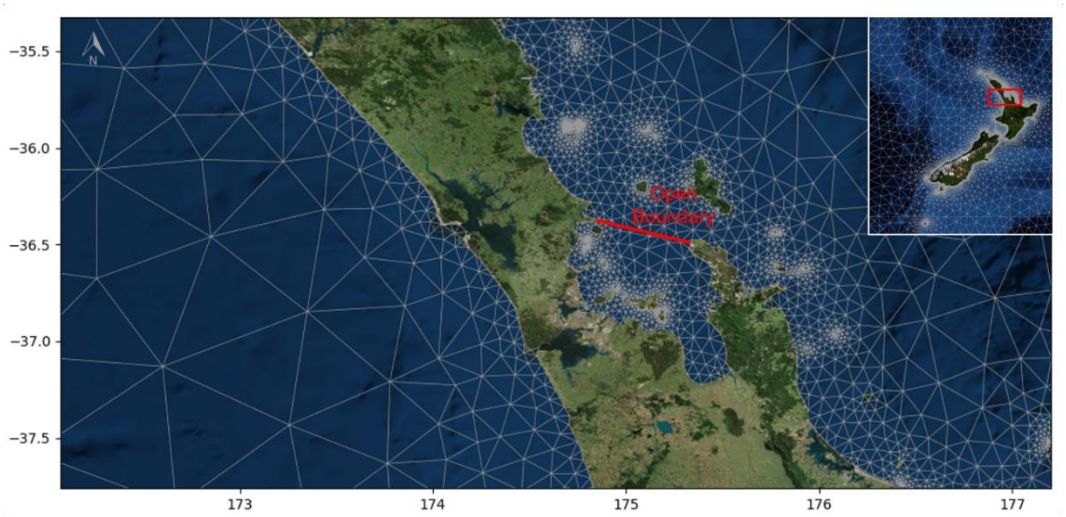

Figure 2-8 Coarse mesh grid used in MIKE 21 SW to provide the spectral wave conditions along the open boundary of the fine Hauraki Gulf wave domain presented in Figure 2-6.

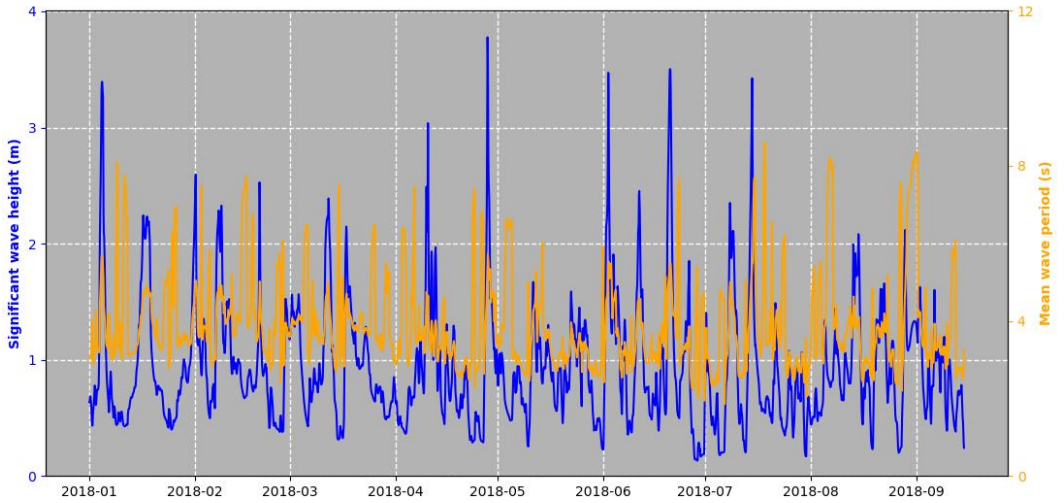

Figure 2-9 Timeseries of the model significant wave height and mean wave period extracted from the NZ wave model at the centre of the open-boundary.

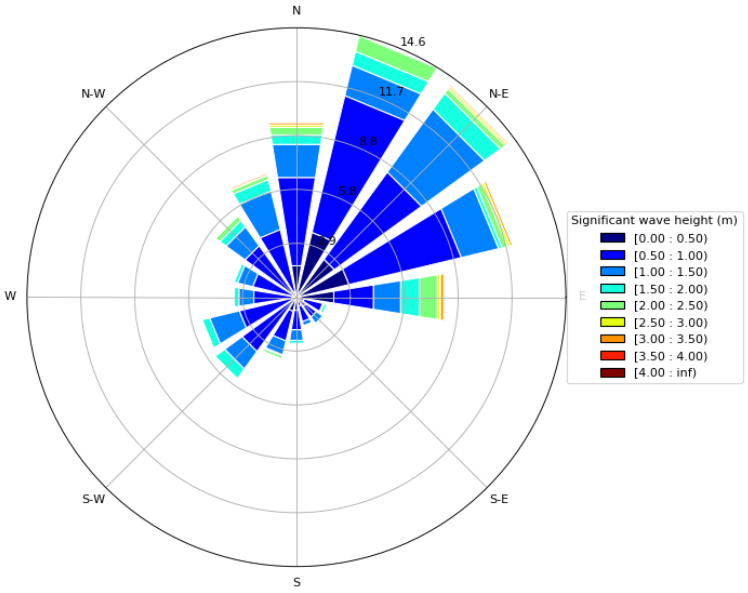

Figure 2-10 Wave rose produced from the NZ wave model data at the centre of the open boundary. between January and October 2018.

2.6 River Discharges

Nineteen discharge locations detailed in Table 2-3 and Figure 2-11 were introduced into the model domain to simulate the inputs of freshwater and suspended sediments associated with the river discharges. Model river flows and SSC were processed combining the river flows provided at 43 sites (Figure 2-11) between 2002 and 2018 by Morphum Environmental (REFERENCE?). Total flows and SSC at the discharge sites in MIKE 3 were calculated adding and weighted-averaging, respectively, multiple catchment discharges provided at 43 sites (Figure 2-11) between 2002 and 2018 (Morphum, 2018). Details of the combination applied to general the MIKE 3 river inputs are given in Appendix A.

Timeseries of river flows and total SSC for all locations are provided in Figure 2-12 to Figure 2-23. Fractions of suspended sand, silt and clay are given in Table 2-4.

Table 2-3 Location and mean statistics of the river discharges over the study area.

Sites	Coordinates (NZTM)		Mean discharge	Mean SSC
	X (m)	Y (m)	(m^3/s)	(kg/m^3)
North Outlet	1756200	5939937	0.0148	0.0014
Awaruku	1756531	5938200	0.0581	0.0040
Long Bay	1756228	5939396	0.0648	0.0048
SS Outer	1755508	5941020	0.0117	0.0014
SS Mid-East	1754826	5940326	0.0151	0.0025
SS Mid-West	1754136	5939807	0.0136	0.0025
SS Inner	1753209	5939603	0.0147	0.0018
Redvale	1752632	5939545	0.2100	0.0032
North Arm	1752638	5940051	0.1055	0.0028
North Shore	1753554	5940505	0.0120	0.0010
Karepiro	1754430	5941714	0.0295	0.0013

Karepiro Beach	1754420	5942375	0.0478	0.0010
Stillwater	1753253	5944226	0.0270	0.0017
Weiti South	1752122	5945383	0.0942	0.0030
Silverdale	1751640	5946341	0.4261	0.0039
Arkle Bay	1756306	5943383	0.0215	0.0020
Whangaparaoa	1754135	5943969	0.0147	0.0020
Weiti North	1753199	5945669	0.0229	0.0020
Duck Creek	1752504	5945430	0.0147	0.0017

Table 2-4 Fractions of suspended sand, silt and clay associated with each river discharge.

Discharge Site	**Mean Fraction**		
	Sand	**Silt**	**Clay**
ArkleBay	0.4%	68.3%	31.4%
WeitiNorth	0.0%	67.8%	32.2%
Silverdale	16.0%	19.3%	64.6%
WeitiSouth	9.9%	39.3%	50.8%
DuckCreek	0.0%	55.9%	44.1%
Stillwater	0.0%	72.5%	27.5%
Karepiro	0.0%	64.4%	35.6%
KarepiroBeach	16.2%	41.5%	42.3%
NorthShore	0.0%	58.1%	41.9%
NorthArm	4.9%	47.3%	47.8%
Redvale	14.5%	41.9%	43.6%
SSInner	0.0%	44.5%	55.5%
SSMidWest	0.3%	52.9%	46.8%
SSMidEast	0.4%	42.2%	57.4%
SSOuter	0.0%	39.7%	60.3%
LongBay	22.9%	8.9%	68.2%
NorthOutlet	0.0%	41.2%	58.8%
Awaruku	0.1%	15.3%	84.6%

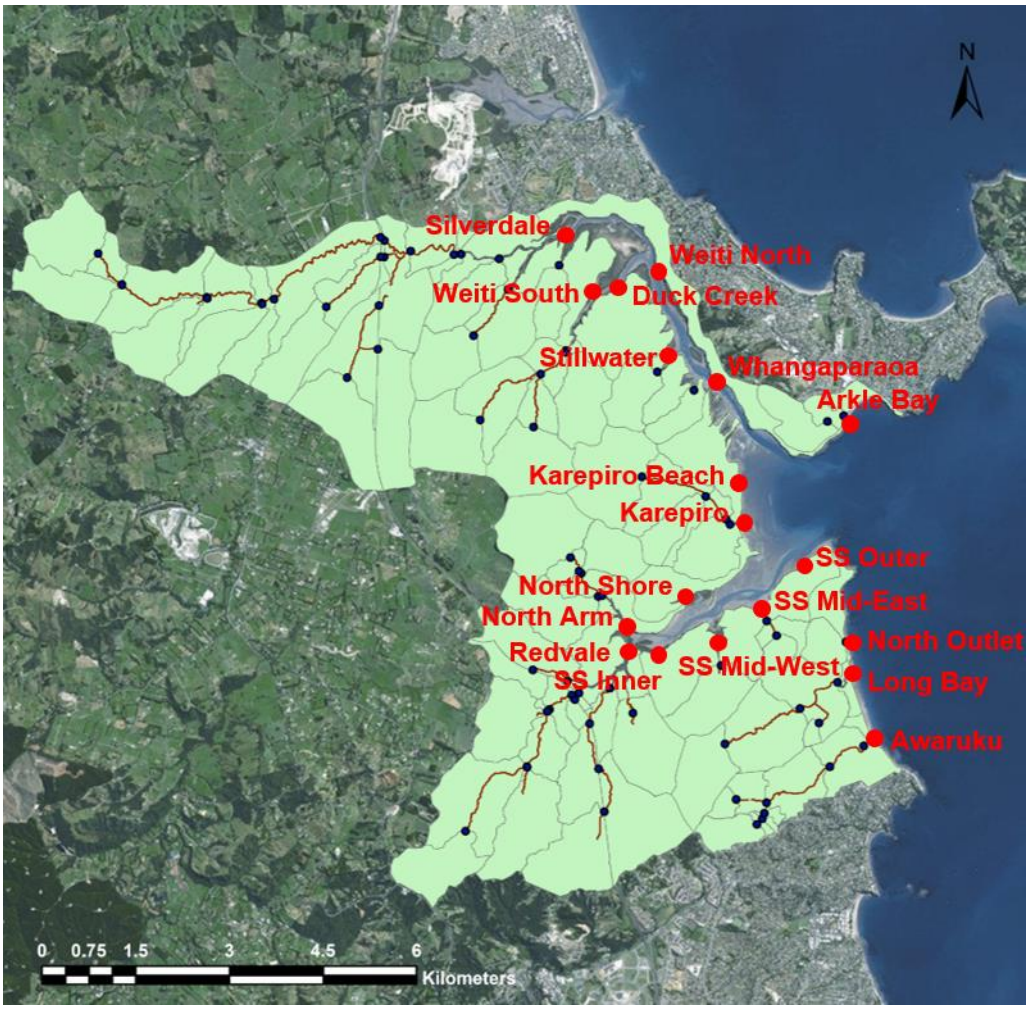

Figure 2-11. Location of the 19 discharge points in Karepiro Bay, Okura River and Weiti River.

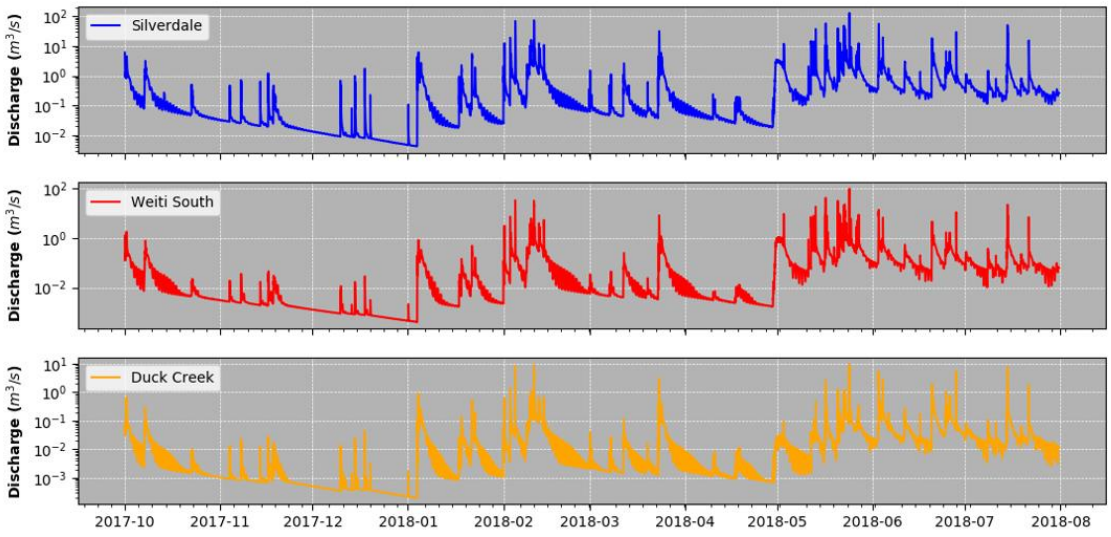

Figure 2-12. River discharges (m^3/s) at the Silverdale, Weiti South and Duck Creek sites between 01/10/2017 and 31/07/2018.

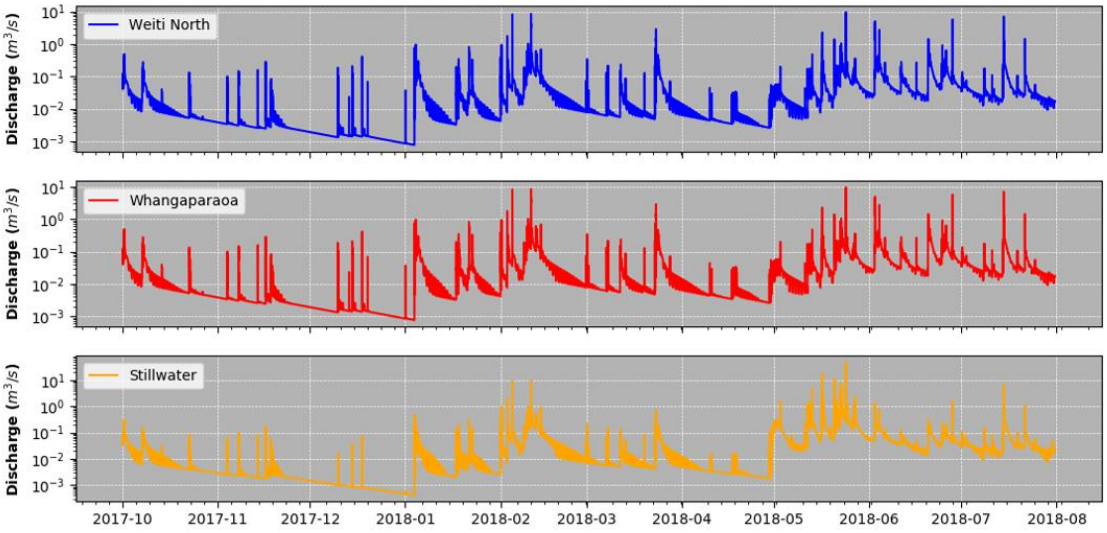

Figure 2-13. River discharges (m^3/s) at the Weiti North, Whangaparaoa and Stillwater sites between 01/10/2017 and 31/07/2018.

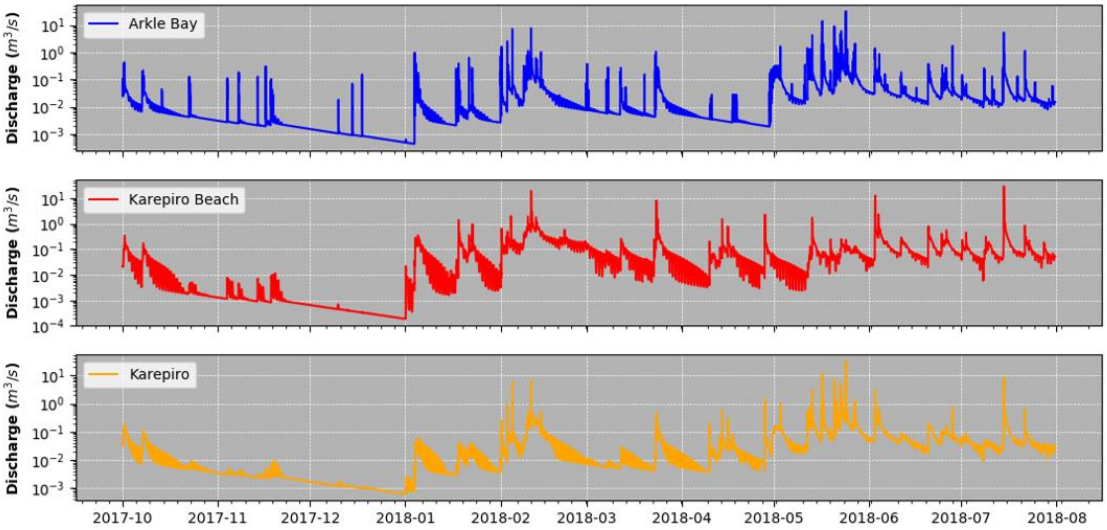

Figure 2-14. River discharges (m^3/s) at the Arkle Bay, Karepiro beach and Karepiro sites between 01/10/2017 and 31/07/2018.

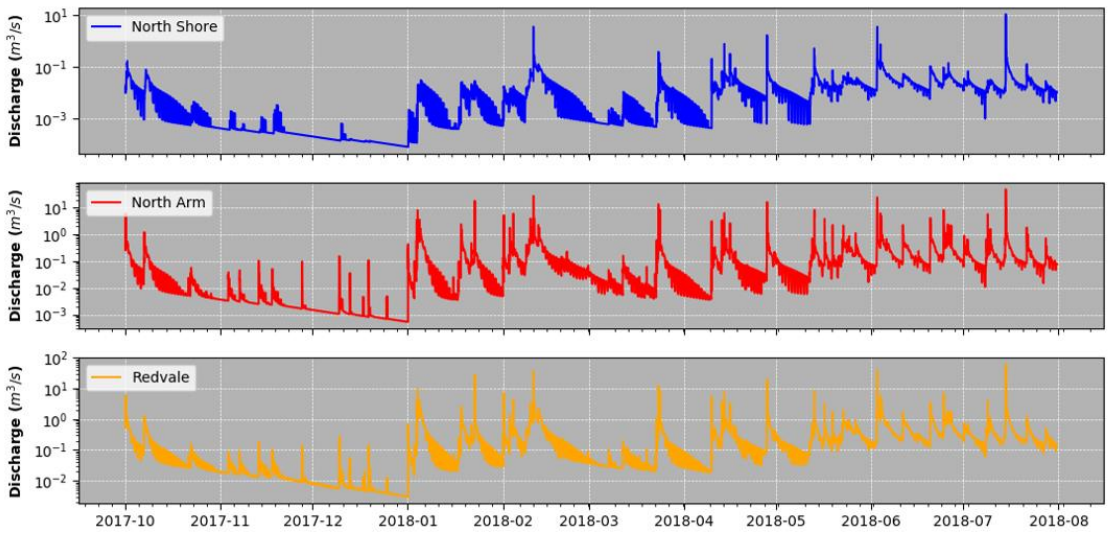

Figure 2-15. River discharges (m^3/s) at the North Shore, North Arm and Redvale sites between 01/10/2017 and 31/07/2018.

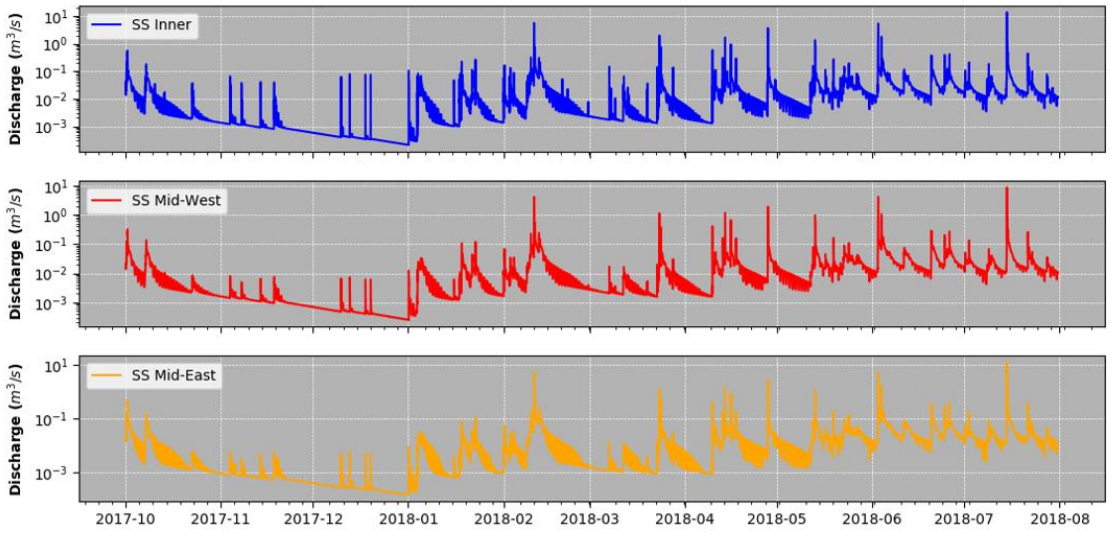

Figure 2-16. River discharges (m^3/s) at the SS Inner, SS Mid-West and SS Mid-East sites between 01/10/2017 and 31/07/2018.

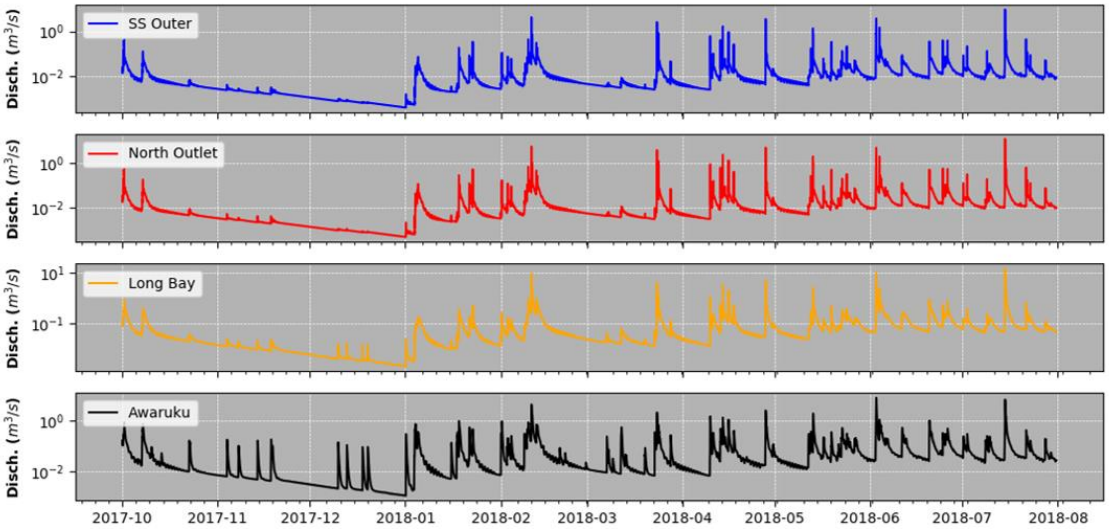

Figure 2-17. River discharges (m^3/s) at the SS Outer, North Outlet, Long Bay and Awaruku sites between 01/10/2017 and 31/07/2018.

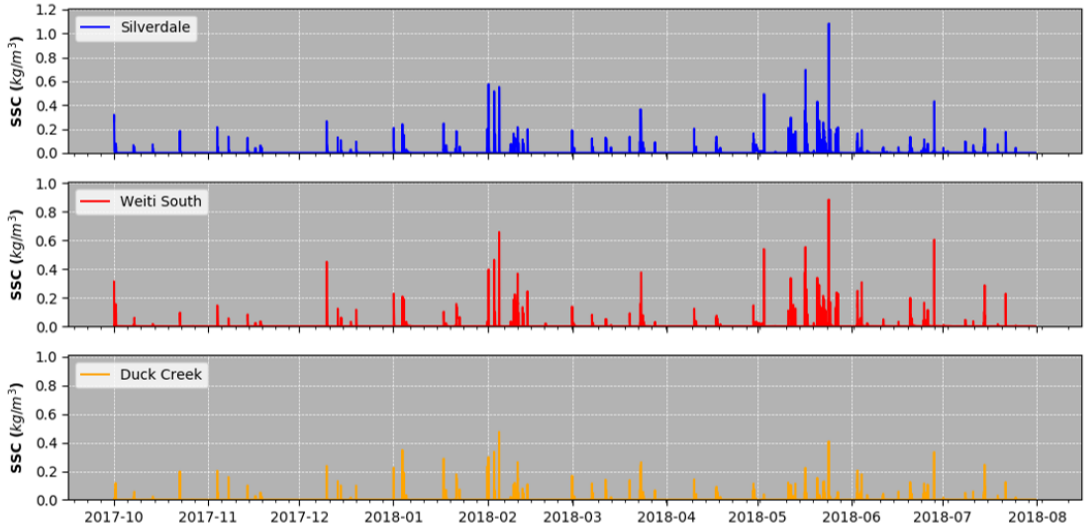

Figure 2-18. Total river suspended sediment concentration (SSC) at the Silverdale, Weiti South and Duck Creek sites between 01/10/2017 and 31/07/2018.

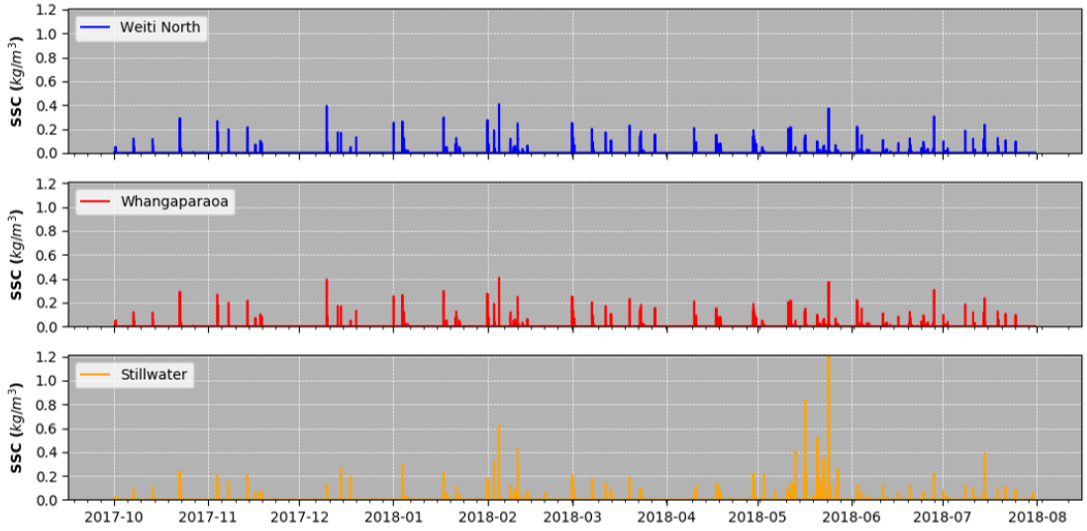

Figure 2-19. Total river suspended sediment concentration (SSC) at the Weiti North, Whangaparaoa and Stillwater sites between 01/10/2017 and 31/07/2018.

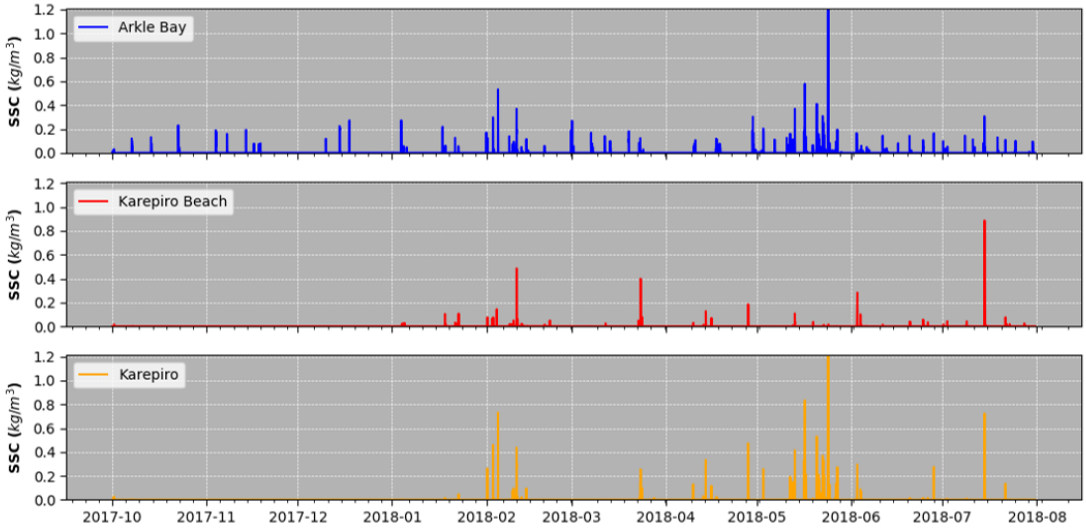

Figure 2-20. Total river suspended sediment concentration (SSC) at the Arkle Bay, Karepiro beach and Karepiro sites between 01/10/2017 and 31/07/2018.

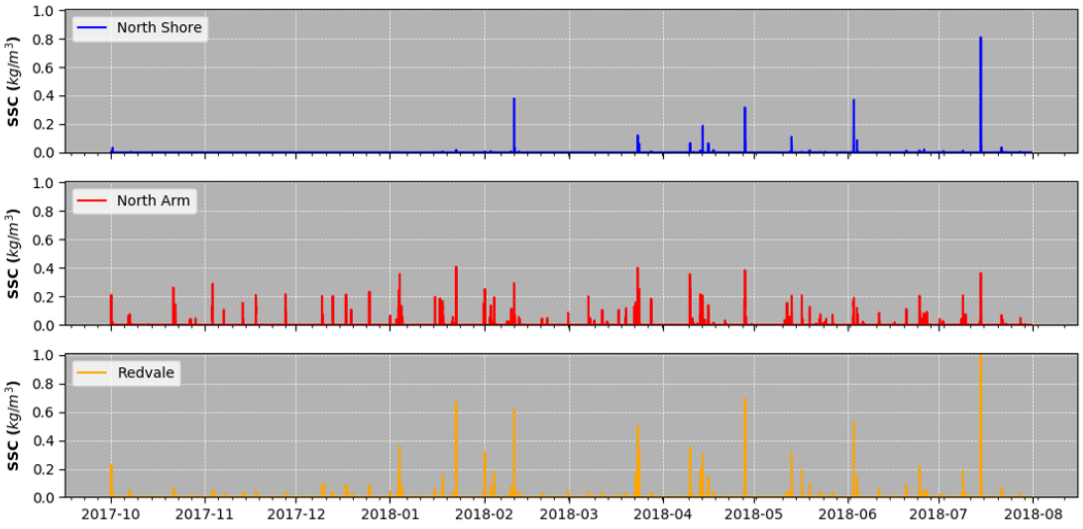

Figure 2-21. Total river suspended sediment concentration (SSC) at the North Shore, North Arm and Redvale sites between 01/10/2017 and 31/07/2018.

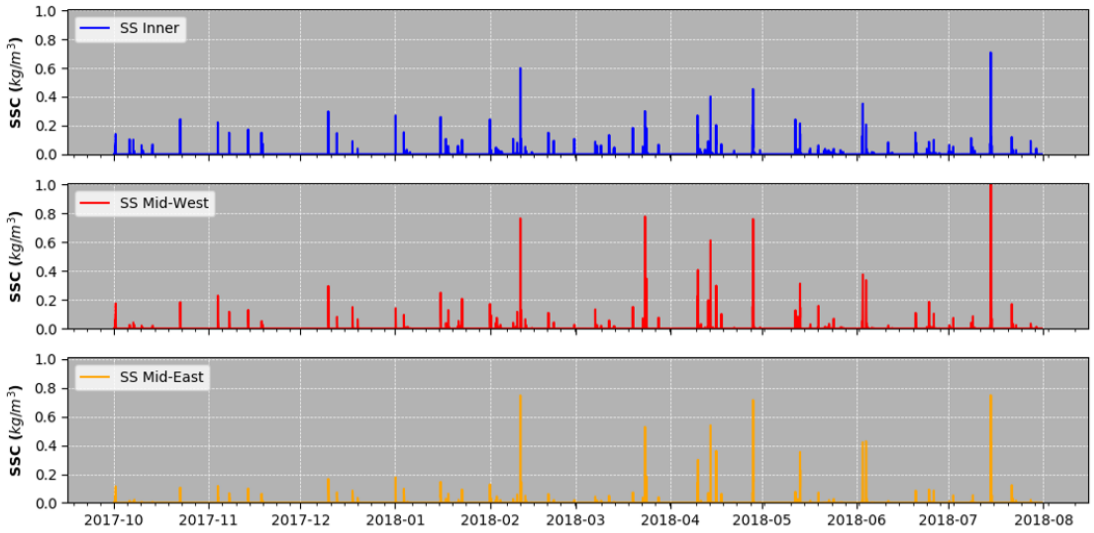

Figure 2-22. Total river suspended sediment concentration (SSC) at the SS Inner, SS Mid-West and SS Mid-East sites between 01/10/2017 and 31/07/2018.

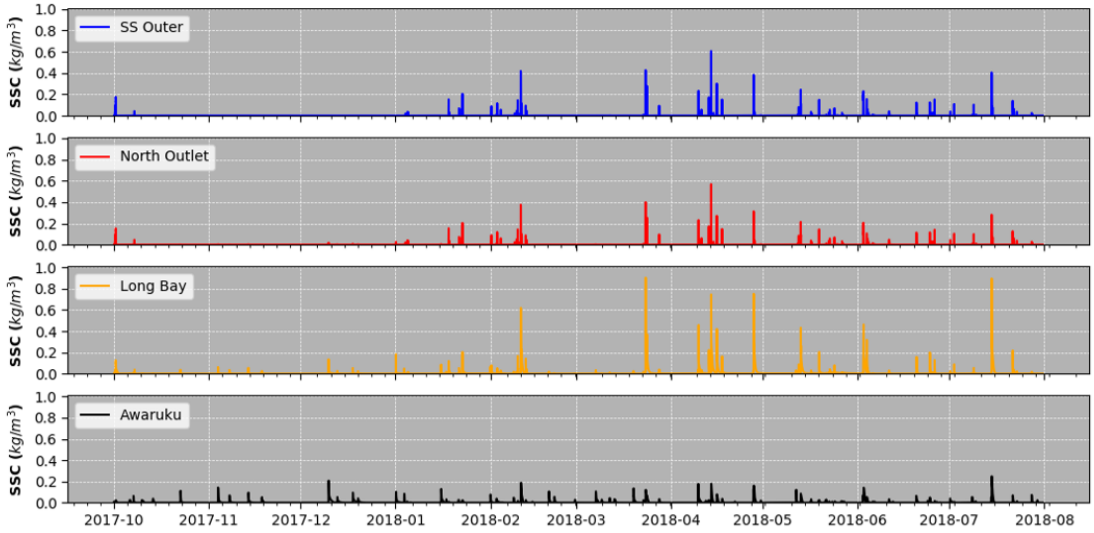

Figure 2-23. Total river suspended sediment concentration (SSC) at the SS Outer, North Outlet, Long Bay and Awaruku sites between 01/10/2017 and 31/07/2018.

2.7 Sea Bed Characteristics

The Mud Transport (MT) module setup has been made based on the analysis of the sediment sampling presented in REFERENCE and the calibration process. Sediment samplings at three positions within Karepiro Bay showed the sea bed was primarily composed of fine sand (>80%) and mud (<20%), with the presence of organic and abundant shell material. The dry density of the muddy-sand in the surface layers was found to be higher than 400 kg/m^3. The dry density of the sea bed combined with the sand-mud-shell mixture highlight a partly consolidated sea bed. Based on this information, the MT model was setup using the Partheniades (1965) formulation for the erosion of dense mud and a unique space-varying bed thickness layer with a constant density of 450 kg/m^3. An erosion coefficient of 0.00014 kg/m^2/s was defined accordingly to the recommended values for dense mud (DHI, 2017d). The power of erosion was increased from the

default value (1) to a calibrated value (1.22). The critical shear stress for erosion was defined in the range 0.125 – 0.425 N/m^2 depending on the bathymetry (Figure 2-24) to represent the space-varying level of consolidation of the sea. The model initial bed thickness was determined combining the bed thickness used in NIWA (Pritchard et al. 2009) with a 3-month morphological spin-up. This approach aimed to avoid unrealistic sediment transport patterns in the shallow areas caused by inconsistencies between the sea bed characteristics and the model forcing. The model initial bed thickness is shown in Figure 2-24.

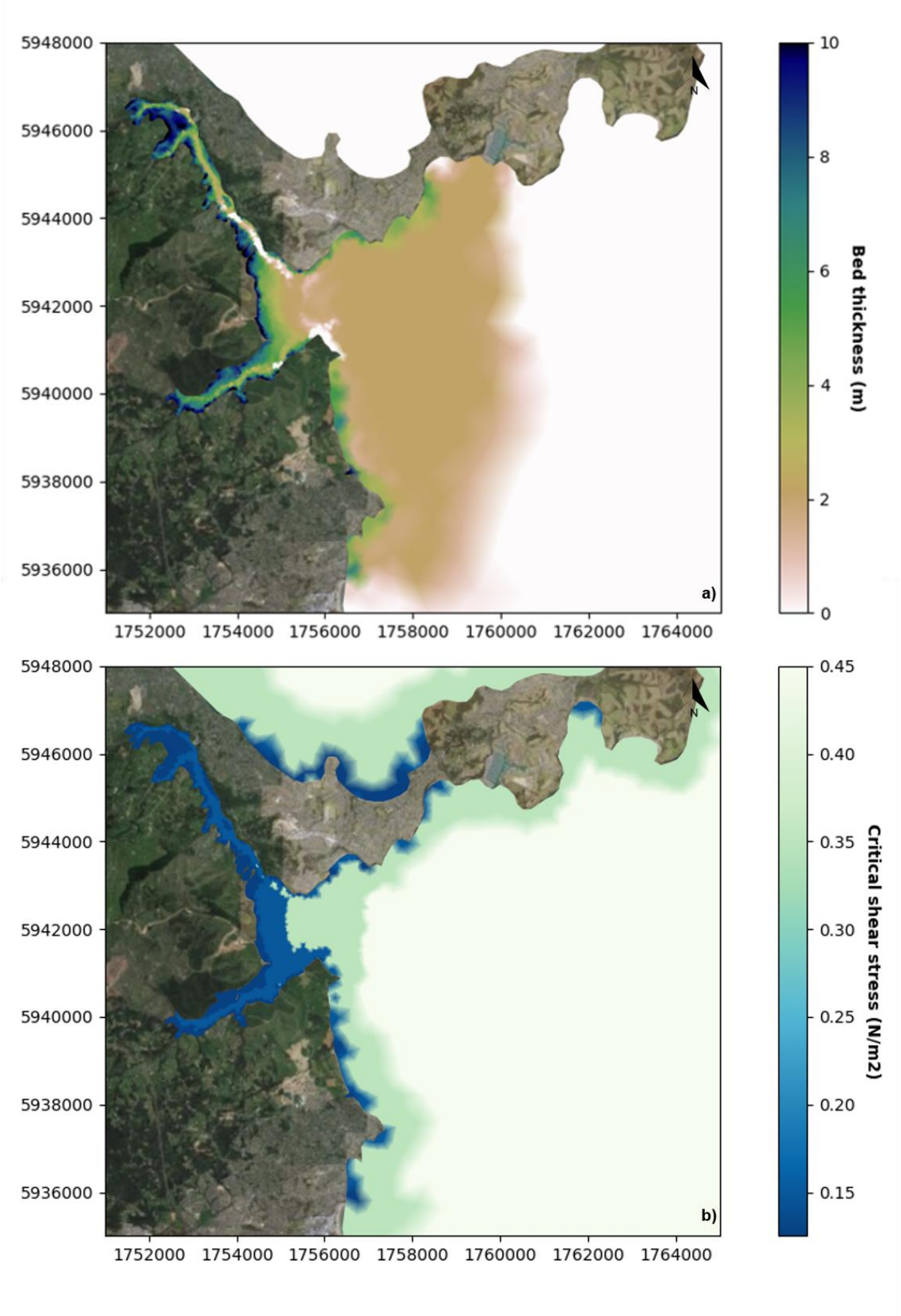

Figure 2-24. Initial bed thickness within the Okura Estuary in the Mud Transport model.

3 Model Validation

To ensure the capability of the model to appropriately simulate the sediment transport in the study area, model outputs were compared against measurements of significant wave heights, water elevations, 3D current velocities, turbidity and bed thickness changes. The main purpose of the validation was to demonstrate the present model was a suitable tool to assess the effect of the discharges from the Weiti and Okura catchments. For this purpose, both hydrodynamics and sediment dynamics were investigated. Results of the validation are presented in this section.

3.1 Waves

Predicting wave heights in semi-enclosed environments such as the Hauraki Bay is challenging as it requires the use of accurate wind conditions to force the spectral wave model. To verify the accuracy of the hindcast, the model significant wave heights were compared against the wave measurements at position AK1 (Figure 3-1) between March and July 2018. As shown in Figure 3-2 and Figure 3-3, the model represents very well the local wind-induced peak wave events characterised by waves higher than 1 m. The 6-hour wind forcing does not allow capturing the rapid variations of the sea state leading to wave heights in the range 10 – 25 cm. However, timeseries of measured bed level changes at the entrance to Karepiro Bay (DHI, 2018) showed that sediment transport was mostly occurring during storm events. The shear stresses induced by 10 – 50 cm waves are therefore negligible in this context.

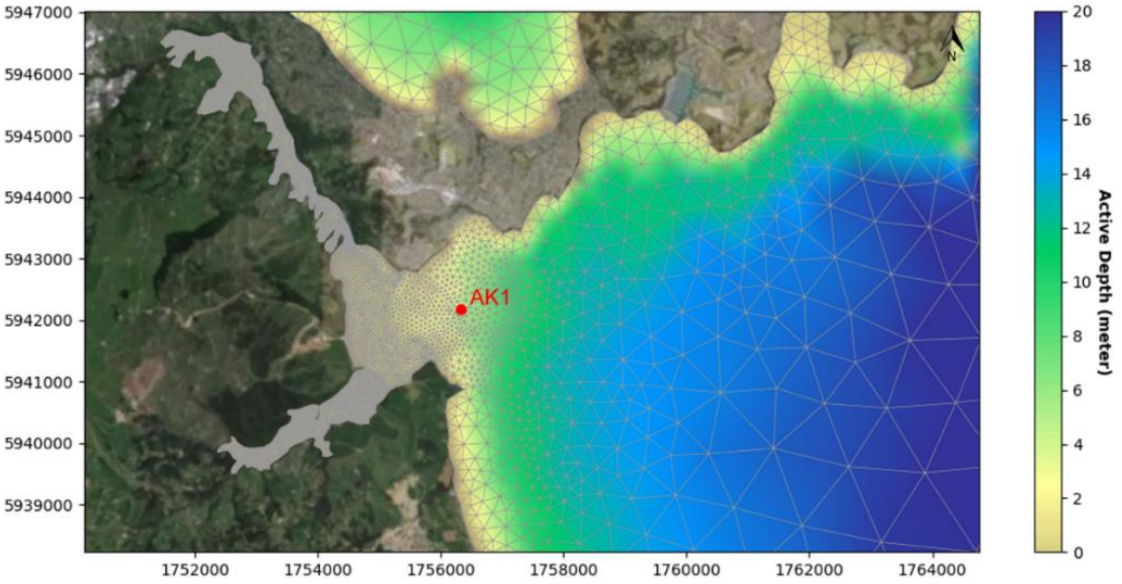

Figure 3-1. Bathymetry map with the location of the ADCP deployed at Position AK1 at the entrance to Karepiro Bay.

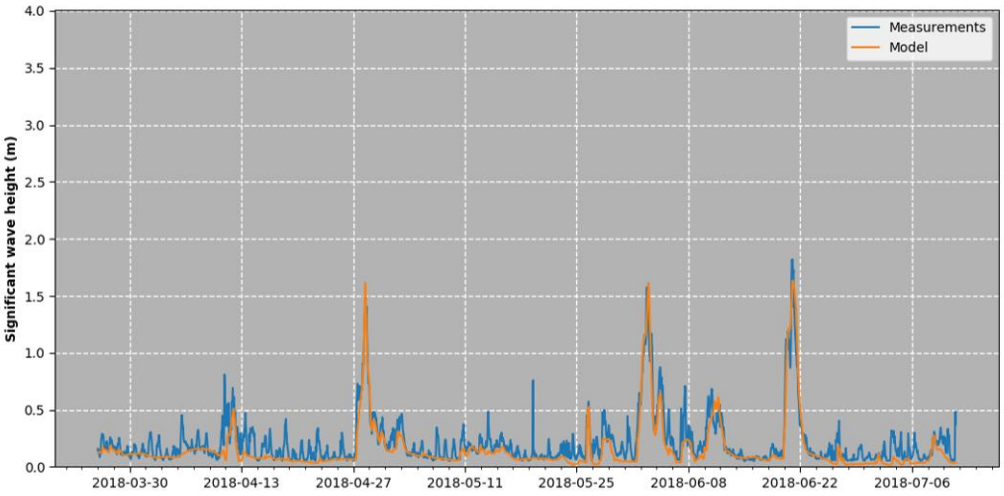

Figure 3-2. Measured and model significant wave heights at Position AK1 at the entrance to Karepiro Bay.

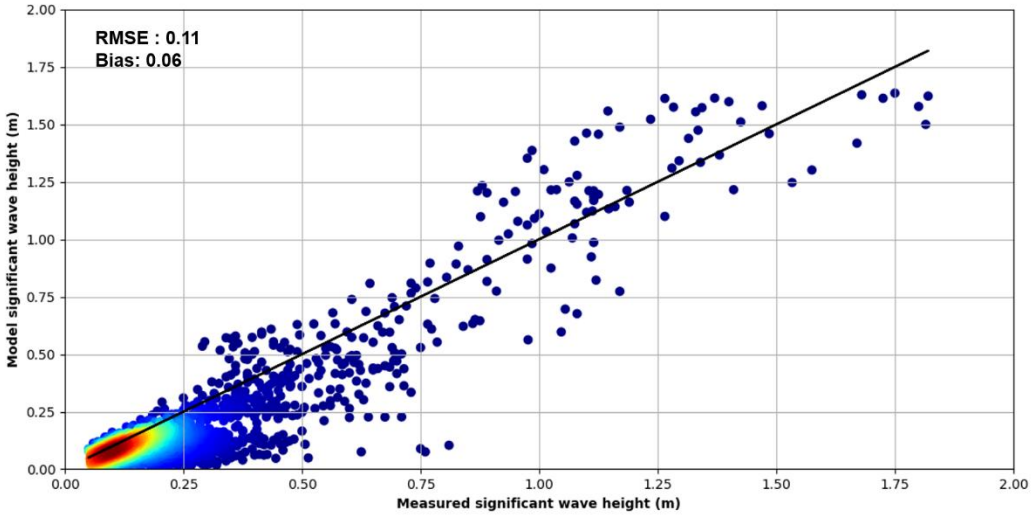

Figure 3-3. Scatter plot produced from measured (X-axis) and model (Y-axis) significant wave heights at Position AK1 at the entrance to Karepiro Bay.

3.2 Water elevation

Comparisons between model and measured water elevation at Position AK2 (Figure 3-4) between March and May 2018 highlights a good level of agreement (Figure 3-5). The maximum difference in water elevation does not exceed 25 cm over the calibration period which corresponds to ~10% of the tidal amplitude. Such feature is important as it determines the capability of the model to realistically simulate the flooding and drying of the inter-tidal areas where significant sediment fluxes occur between the rivers and Karepiro Bay.

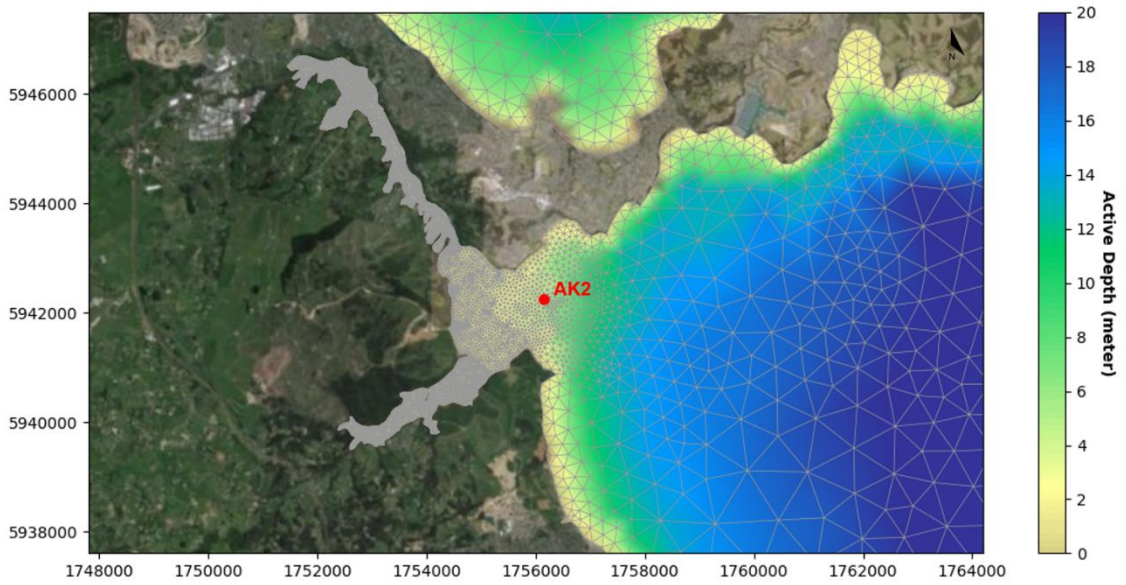

Figure 3-4. Bathymetry map with the location of the instrument deployed at Position AK2 to measure water elevation.

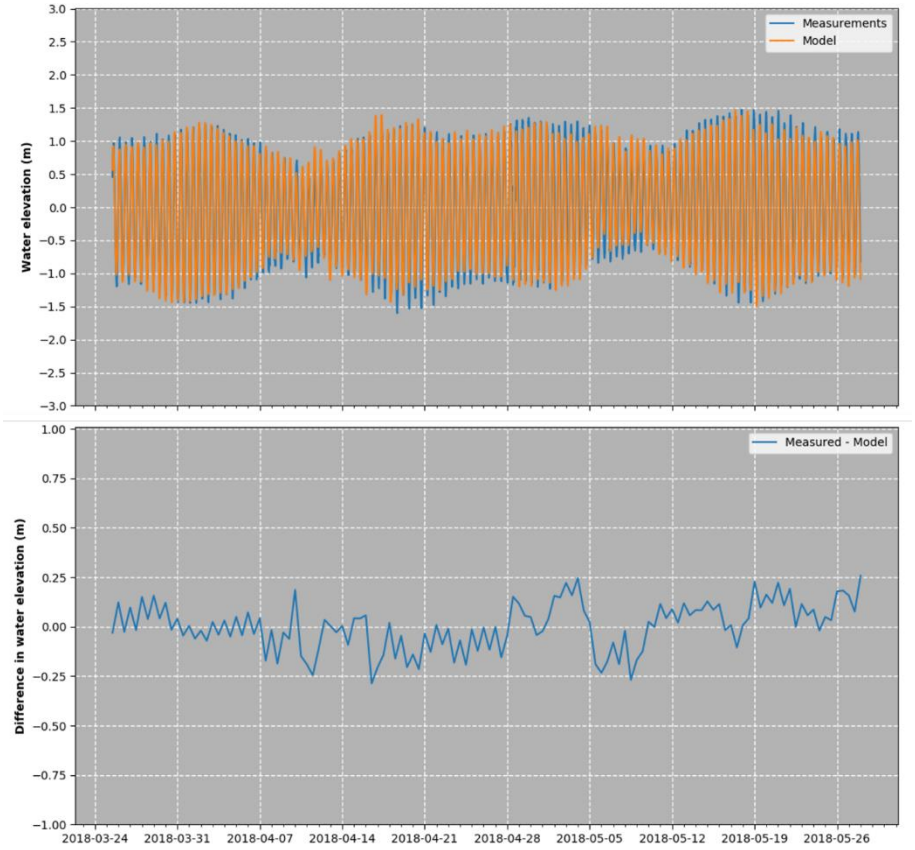

Figure 3-5. Measured and model water elevations (top panel) and differences in water elevation (bottom panel) at Position AK2.

3.3 Currents

To complete the validation of the hydrodynamic model, near-surface, mid-depth and near-bottom currents were compared against the measured data at position AK1 between March and July 2018. Current speeds and directions were examined at these levels to ensure the model allows capturing the combining effect of tides, winds and bed roughness on the local hydrodynamics. Timeseries, Quantile-Quantile (QQ) plot and current roses are provided for each level in Figure 3-6, Figure 3-7 and Figure 3-8.

The validation results indicate the model satisfactorily simulate the hydrodynamics in Karepiro Bay. The QQ plots highlight close distributions of current speed through the water column. Velocities are somewhat under-estimated in surface (<20%) and at mid-depth (<10%), and over-estimated near bottom (<10%). Model current directions are also consistent with the measurements. We can, however, note a ~10 – 20° shift in the tidal ellipse which is not expected to significantly modify the sediment transport patterns.

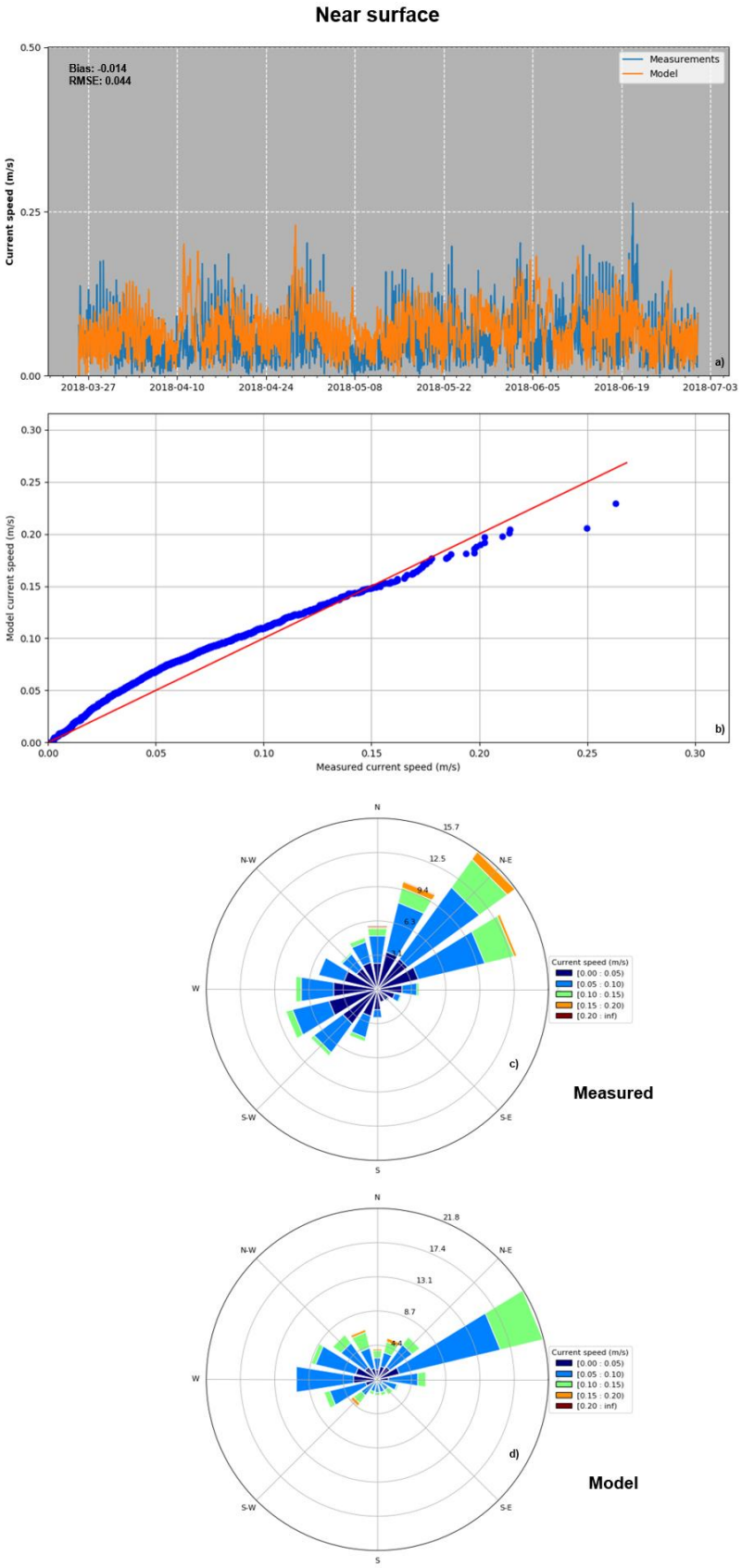

Figure 3-6. Measured and model near-surface current timeseries, Quantile-Quantile plot and roses.

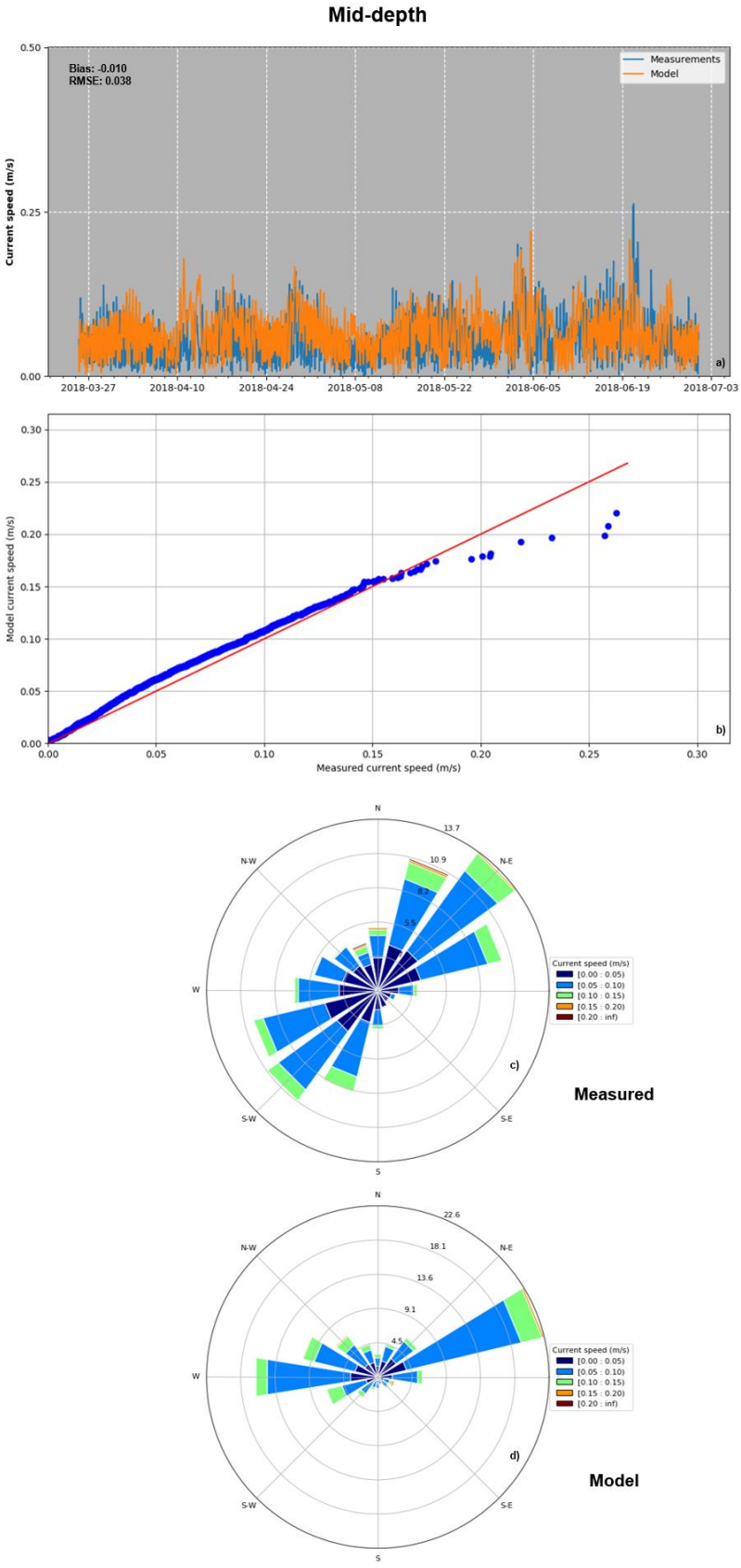

Figure 3-7. Measured and model mid-depth current timeseries, Quantile-Quantile plot and roses.

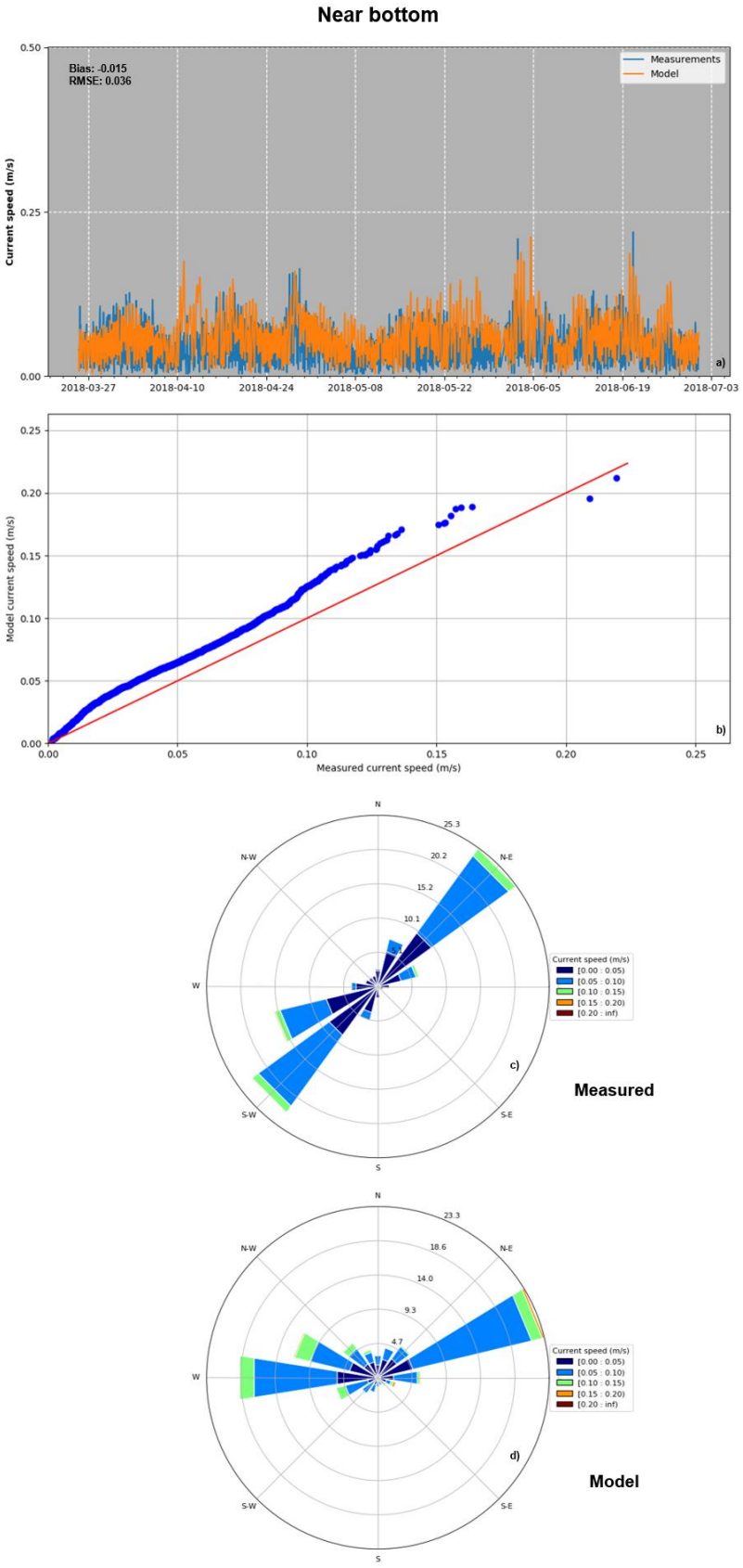

Figure 3-8. Measured and model near-bottom current timeseries, Quantile-Quantile plot and roses.

3.4 SSC/Turbidity

In absence of calibration of the turbidity – SSC relationship, the predicted SSC were normalized and compared against the measured turbidity to qualitatively assess the sediment transport model.

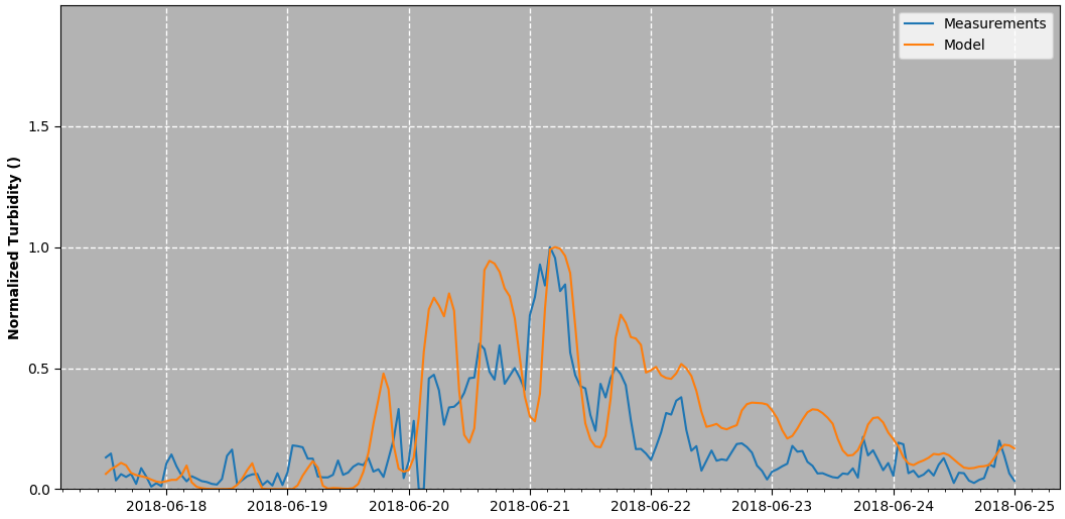

Figure 3-9. Measured and model normalized turbidity at Position AK2AMR during one event characterised by significant deposition. In absence of calibration ratio NTU:SSC, timeseries were normalized using the maximum value.

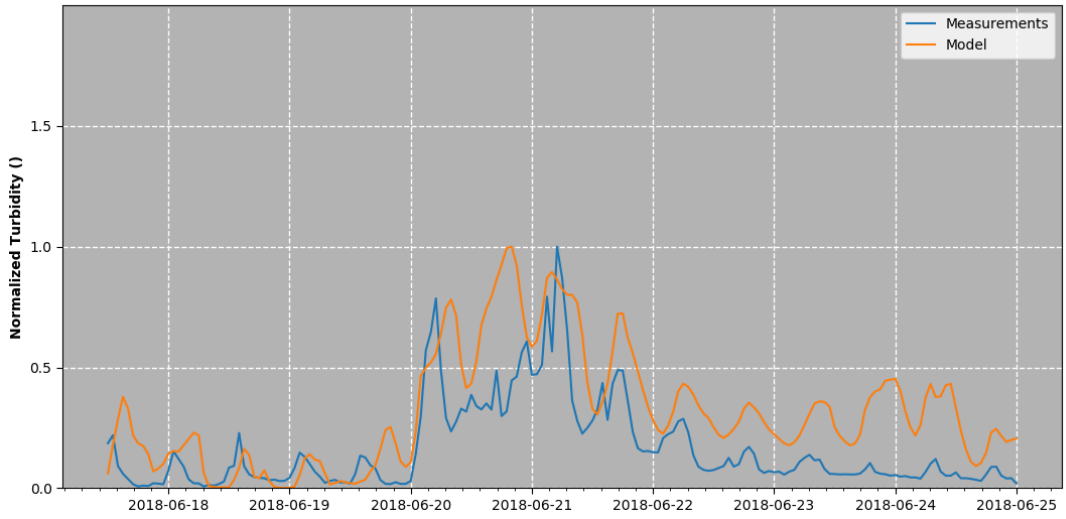

Figure 3-10. Measured and model normalized turbidity at Position AK3A during one event characterised by significant deposition. In absence of calibration ratio NTU:SSC, timeseries were normalized using the maximum value.

4 Representative period

Based on an analysis of the long-term data from Morphum and the Whangaparoao wind record a representative period was chosen to run the calibrated coupled model. This period was chosen to ensure that predicted deposition rates could be related to annual accumulation rates and that predicted suspended sediment concentrations occur for a broad range of sediment inputs, wind and wave conditions.

It was found that the first 6 months of 2018 provided such conditions.

Figure 4-1 shows the weekly and accumulated sediment load for the period between January and July 2018. For context, the average weekly load delivered to the system is 433 tonnes (or an equivalent average annual load 2261 tonnes.

Figure 4-2 shows the scatter plot of the weekly mean freshwater inflow (for all the catchment outlet) and total sediment load from all the catchment outlets from the full Morphum data (2002-2018). Also shown in the scatter plot of the weekly mean freshwater inflow (for all the catchment outlet) and total sediment load from all the catchment outlets from the Morphum data for the first 6 months of 2018. It can be seen that the inputs for the 2018 period are very representative of the longer term distribution for medium to higher flows and loads but does not include periods of low flows and loads.

Data in Table 4-1 shows the weekly flow and load data and the rank of each of the weeks based on the full Morphum dataset. The representative period chosen contains 6 events ranked in the top 30 of weekly loads.

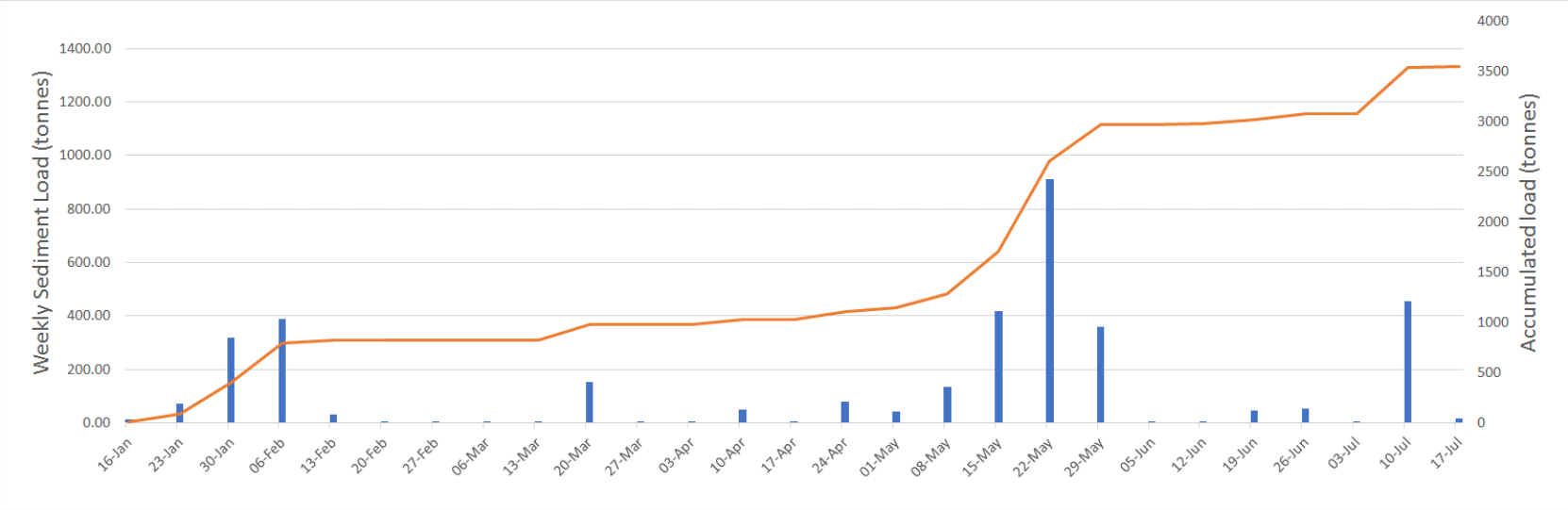

Figure 4-1. Time-series of weekly sediment load and accumulated sediment load for the first 6 months of 2018.

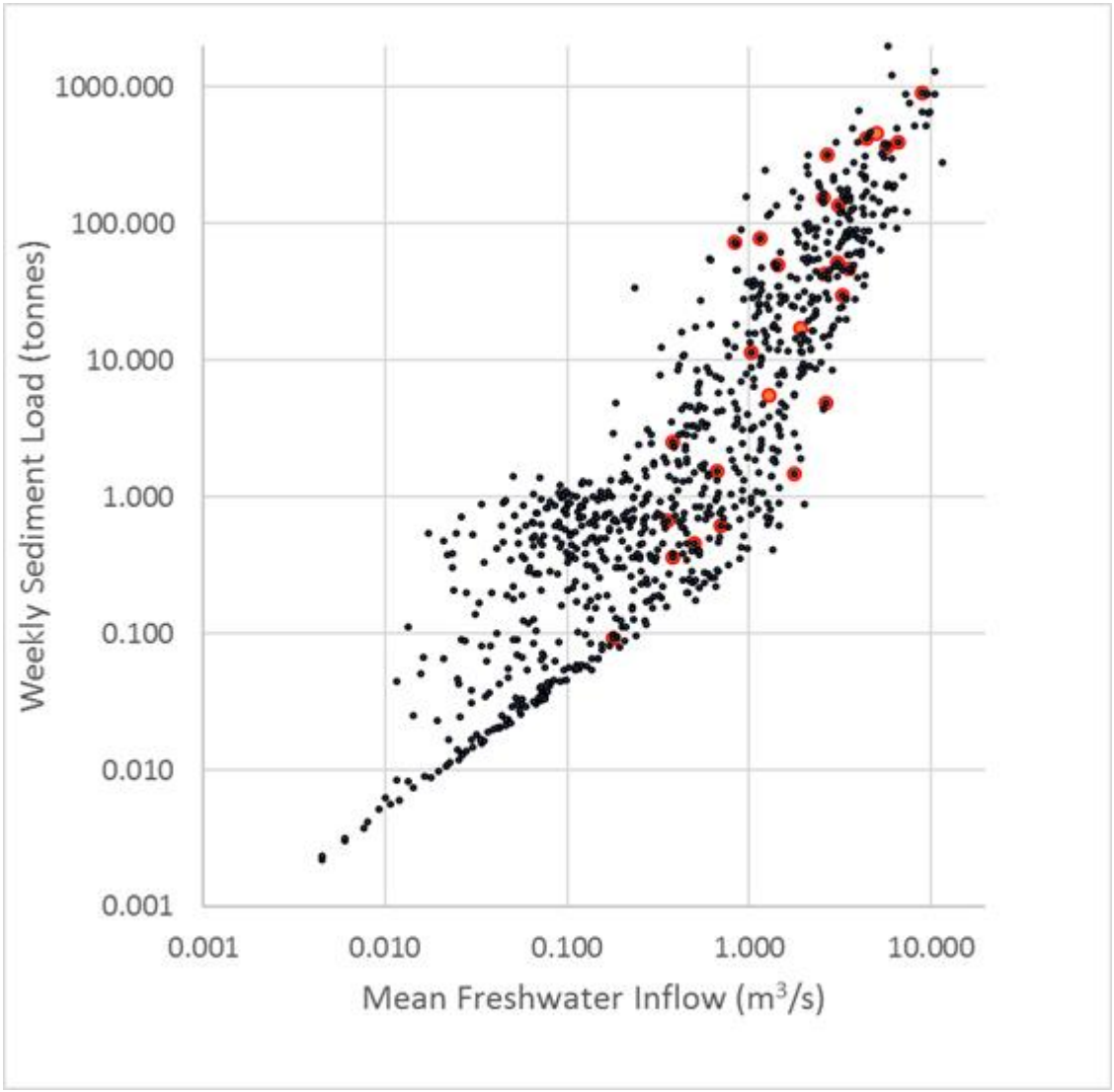

Figure 4-2. Scatter plot of weekly mean freshwater flow and sediment delivery for the full FWMT record from January 2002-July 2018 (black symbols) and for the 6 month period from January 2018 (red symbols).

Table 4-1 Summary of weekly load and flow data from the first 6 months of 2018.

Week beginning	Mean freshwater inflow (m^3/s)	Sediment delivered (tonnes)	Rank from full record January 2002-July 2018*	
16/01/2018	1.023	11.39	261	
23/01/2018	0.836	73.04	124	Lower Wind, NW
30/01/2018	2.677	316.78	29	Moderate Wind, SW
6/02/2018	6.624	389.92	23	Stronger Wind, SW
13/02/2018	3.257	29.99	186	Moderate Wind, SW
20/02/2018	0.699	0.61	547	
27/02/2018	0.355	0.68	525	
6/03/2018	0.383	2.49	352	
13/03/2018	0.383	0.36	630	
20/03/2018	2.547	154.00	67	Moderate Wind, SW
27/03/2018	0.502	0.46	586	
3/04/2018	0.179	0.09	737	
10/04/2018	1.432	49.40	150	Stronger Wind, NE
17/04/2018	0.665	1.53	387	
24/04/2018	1.153	78.31	118	Moderate Wind, SW
1/05/2018	2.622	43.07	163	Lower Wind, NE
8/05/2018	3.129	134.91	75	Lower Wind, SE
15/05/2018	4.446	417.52	20	Stronger Wind, SE
22/05/2018	8.893	910.30	4	Stronger Wind, NE
29/05/2018	5.682	358.60	26	Moderate Wind, NW
5/06/2018	2.659	4.83	307	
12/06/2018	1.771	1.49	391	
19/06/2018	3.555	46.34	155	Lower Wind, NW
26/06/2018	3.078	52.38	146	Moderate Wind, NE
3/07/2018	1.281	5.51	303	
10/07/2018	5.070	455.38	18	
17/07/2018	1.910	17.24	228	Stronger Wind, NE

5 Summary of Model Setup

Table 5-1 provides an overview of calibration parameters and setup of the calibrated coupled model in the context of the NIWA model (Pritchard et al., 2009).

Table 5-1. Summary of NIWA model setup and coupled model calibration parameters and setup.

DHI MIKE3 FM	Parameter	Pritchard et al. (2009)	DHI (2019)
Model Simulation time		10 days	6 months
Bed roughness	Z0	0.05	
Horizontal mixing **Lower limit** **Upper limit**	Smagorinsky coefficient	0.28 1.8e-006 m^2/s 10 m^2/s	0.28 0.1 100
Vertical mixing	C_{my} C_{1e} C_{2e} C_{3e} Prandtl number Turbulent kinetic energy Dissipation of turbulent kinetic energy	0.09 1.44 1.92 0 0.9 1.0 1.2	0.09 1.44 1.92 0 0.9 1.0 1.3
Salinity scaling factor		1.1	1.0
Wind drag coefficient			
Bed erosion	Erosion rate ($kg/m^2/s$) Power term	6e-005 4.3	5e-005 4.3
Erosion critical shear stress	ρ_e	Constant 0.2 N/m^2	Spatially varying 0.125 N/m^2 Inter-tidal areas 0.150 N/m^2 Sub-tidal areas 0.425 N/m^2 Offshore
Deposition critical shear stress	ρ_d	0.1 N/m^2	0.1 N/m^2
Number of catchment sources		4	20
		Scaled flow and SSC from Awanohi data Trapezoidal hydrograph and associated SSC time-series	Calibrated FWMT outputs (flow and three grain size SSC) at 15 minute interval,
Grain sizes considered		Three grain sizes modelled independently (assuming all load is associated with an individual grain size) with a constant fall velocity 4 µm (“washload”) 15 µm (fine silt, 0.0002 m/s fall velocity)	Three grain sizes modelled together accounting for flocculation processes Fine silt (mean fall velocity = 0.00002 m/s) Coarse silt (mean fall velocity = 0.0021 m/s)

		40 µm (coarse silt)	Fine sand (fall velocity = 0.001 m/s)
Wave forcing		None	Full spectral wave model
Tidal boundary condition		Sinusoidally varying synthetic tide representing a spring or neap tide	Broad scale tidal forcing from tidal analysis of Port Charles tide record with inclusion of wind effects
Wind Conditions		Fixed wind of 7.5 m/s from the south-west and calm winds	Spatially varying wind speed and direction validated against observations
Existing bed sediments		Pre-existing estuarine bed sediment not allowed to move	Spatially varying bed thickness representative of observed sediments in the surface mixed layer

6 Example Model Outputs

This section of the report provides typical outputs from the fully coupled model. Results presented here are for the period towards the end of May 2018 which corresponded to a period of higher wave activity (Figure 3-2) and higher sediment load delivery (Section 4).

A separate report will be providing that provides an overview of model outputs for the representative period for the Current State and Future State scenarios being considered (Table 2-1). The form of the output will include spatial maps of key results and time-series data at key sites (to be confirmed).

The predicted currents during the peak outgoing (ebb) and incoming (flood) tide are shown in Figure 6-1 and Figure 6-2 respectively. Note that, for ease of visualisation, the vectors are interpolated onto a regular grid.

The predicted bed shear stress during the peak outgoing (ebb) and incoming (flood) tide are shown in Figure 6-3 and Figure 6-4. The areas of higher bed shear stress give an indication of the areas where the deposition of sediment will be transient. Under waves, the bed shear stress in the area offshore of the entrances to the Okura estuary and Weiti River increases (Figure 6-5). This gives an indication of the role of waves in resuspending existing bed sediments.

Figures 6-6 to 6-8 show the mean suspended sediment concentration (over the duration of he May event) in the top layer of the model, mid water column and near bed.

The pattern of deposition over the duration of the May simulation is shown in Figure 6-9. This figure shows areas where higher deposition rates occur although the net change in bed level also depends on the predicted erosion rate. Figure 6-10 shows the spatial distribution of the predicted erosion rate over the period of the May simulation. The processes sediment delivery from the catchment, resuspension of existing bed sediments and the net deposition and erosion over the duration of the simulation results in the predicted bed level change shown in Figure 6-11.

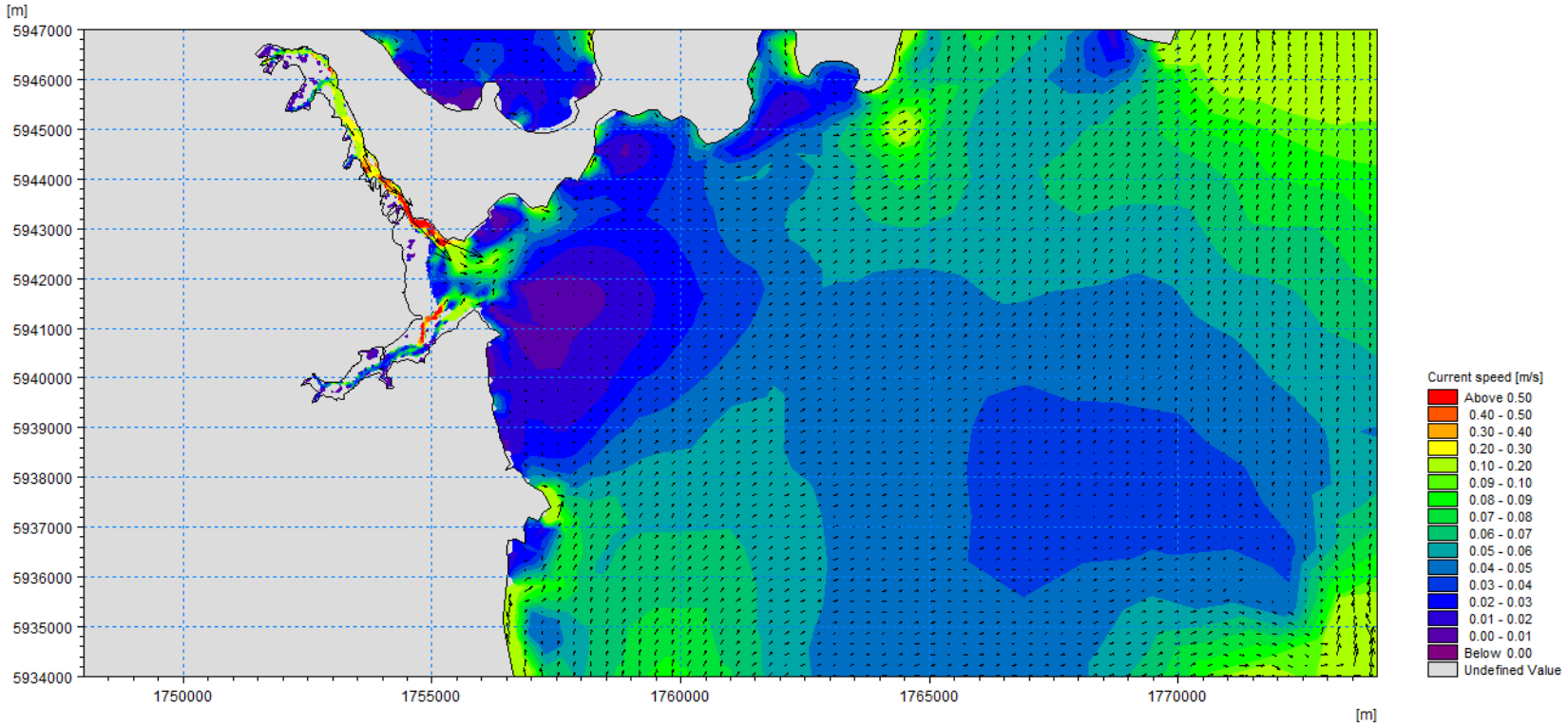

Figure 6-1. Peak ebb (outgoing) tidal currents.

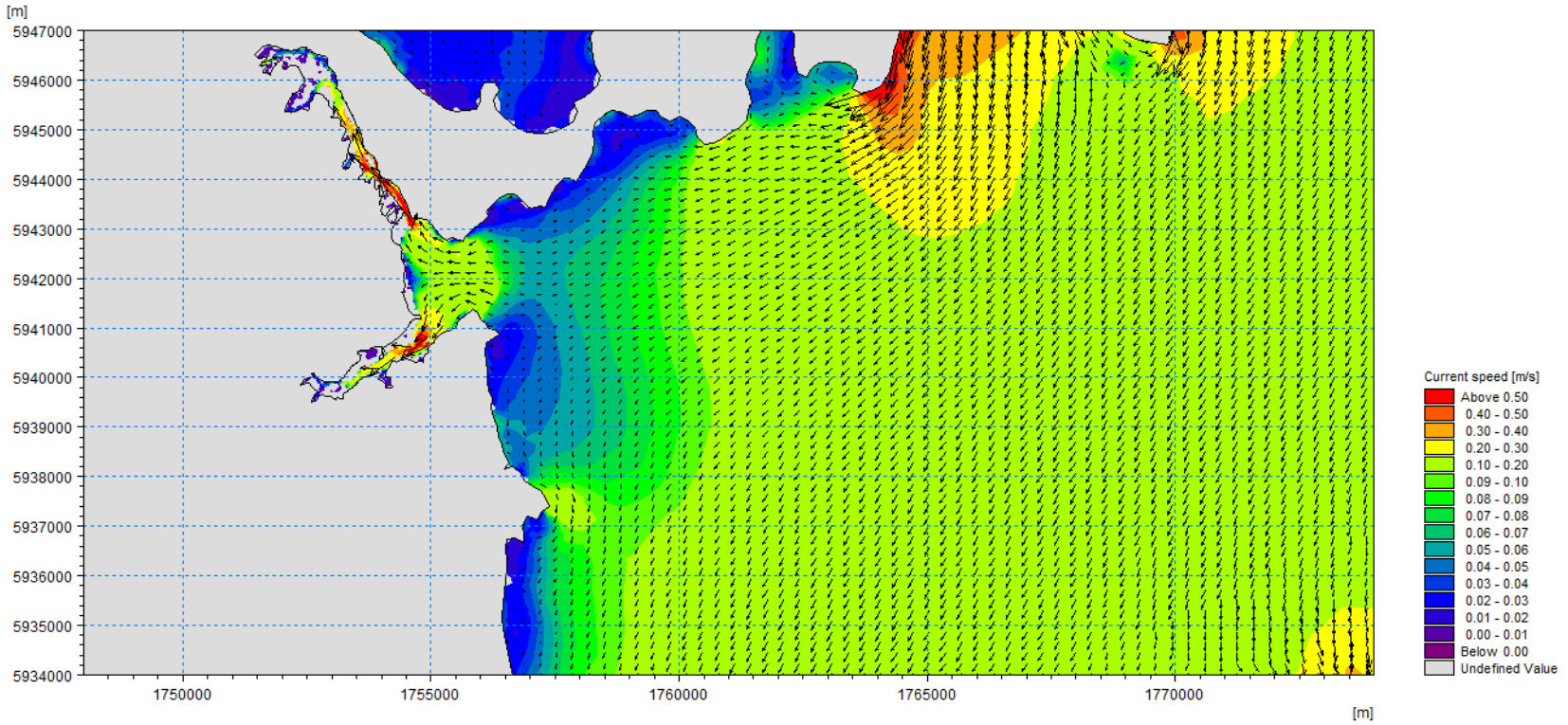

Figure 6-2. Peak flood (incoming) tidal currents.

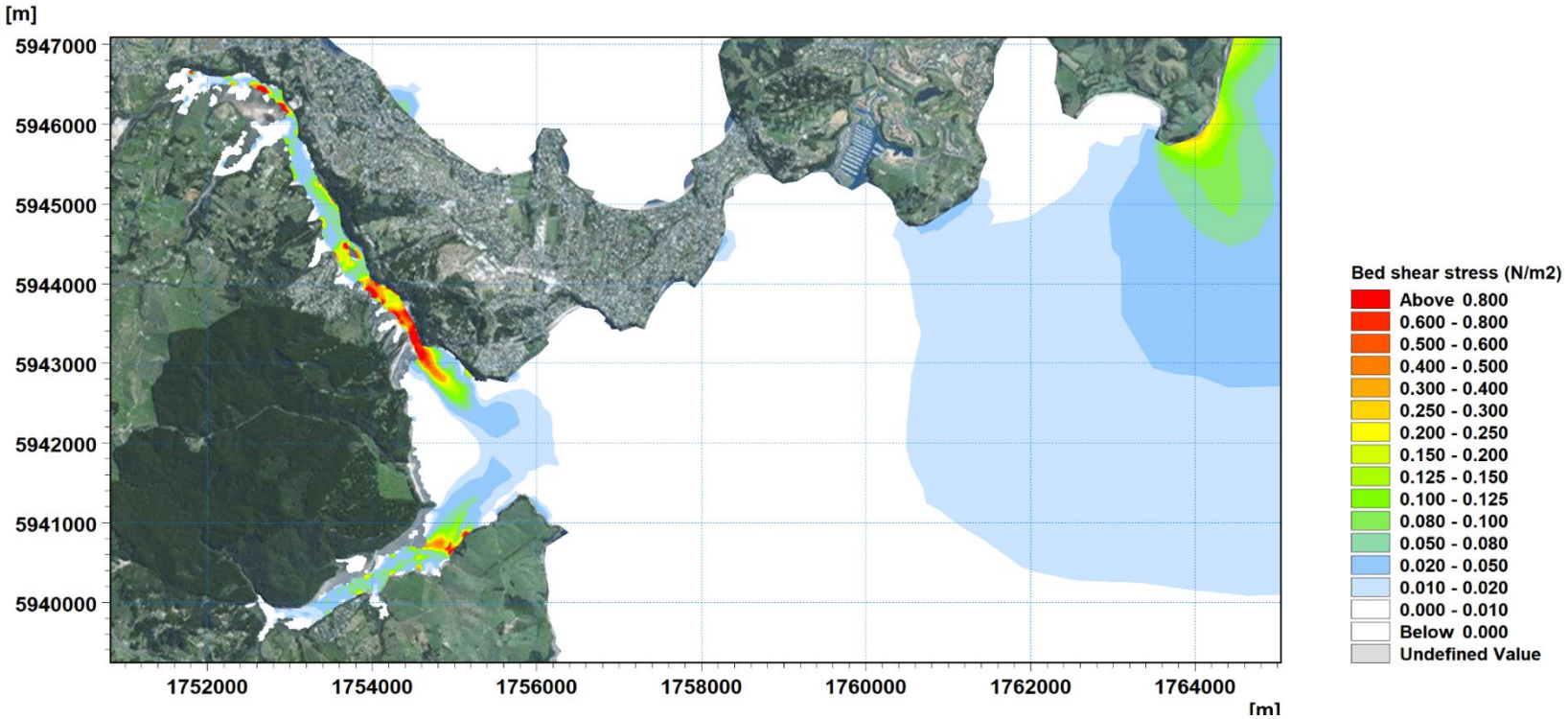

Figure 6-3. Predicted bed shear stress during peak outgoing (ebb tide) during period of low waves.

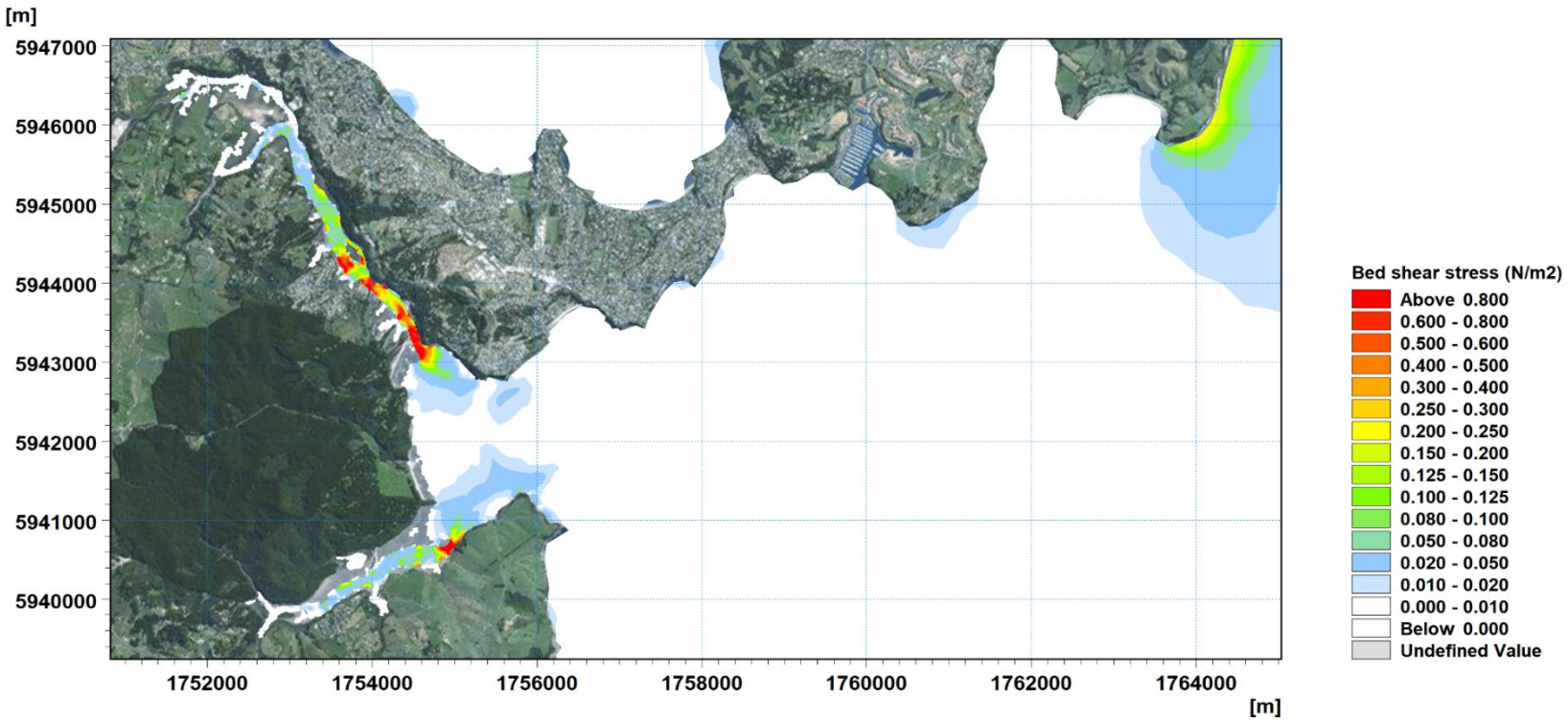

Figure 6-4 Predicted bed shear stress during peak incoming (flood) tide during period of low waves.

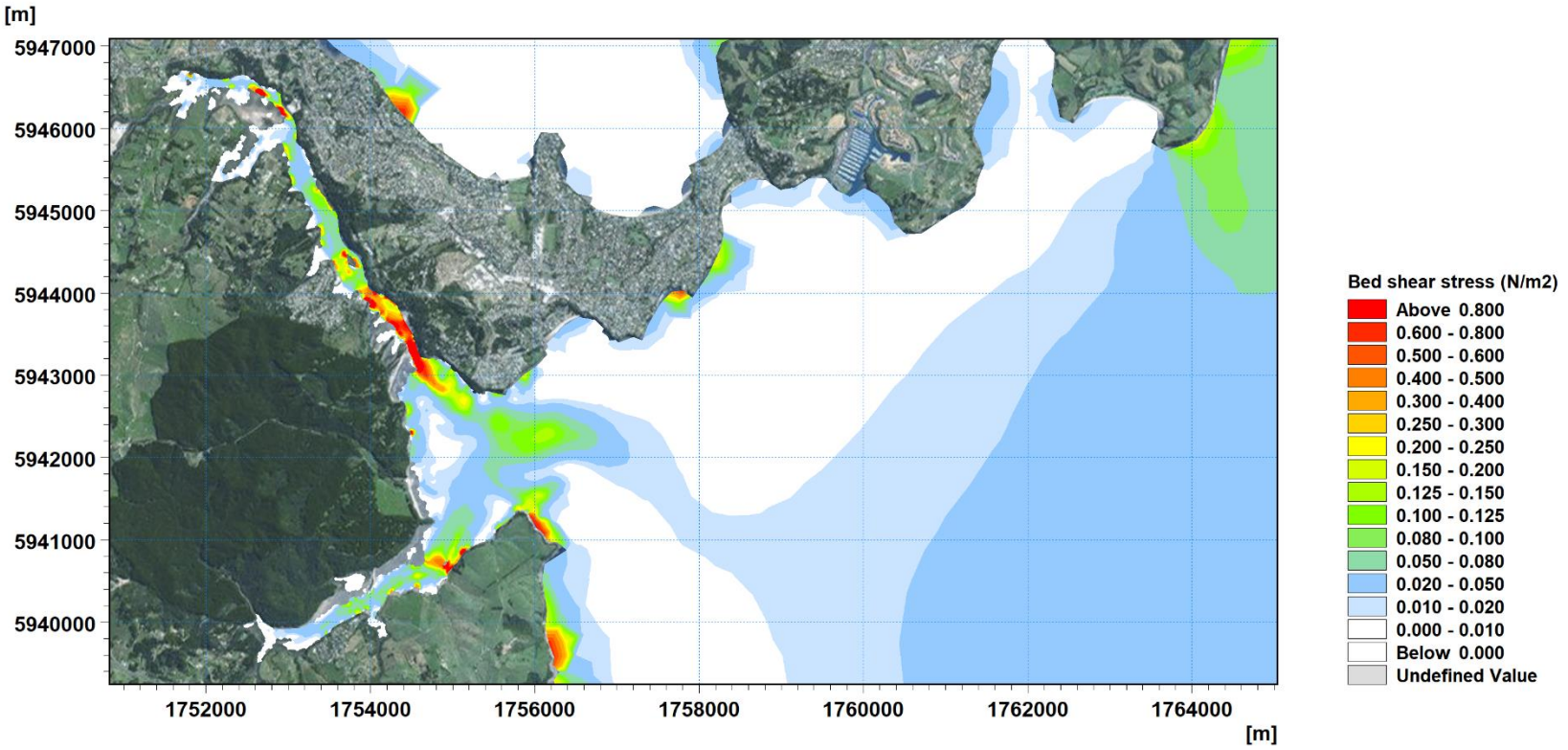

Figure 6-5. Predicted bed-shear stress under moderate wave activity.

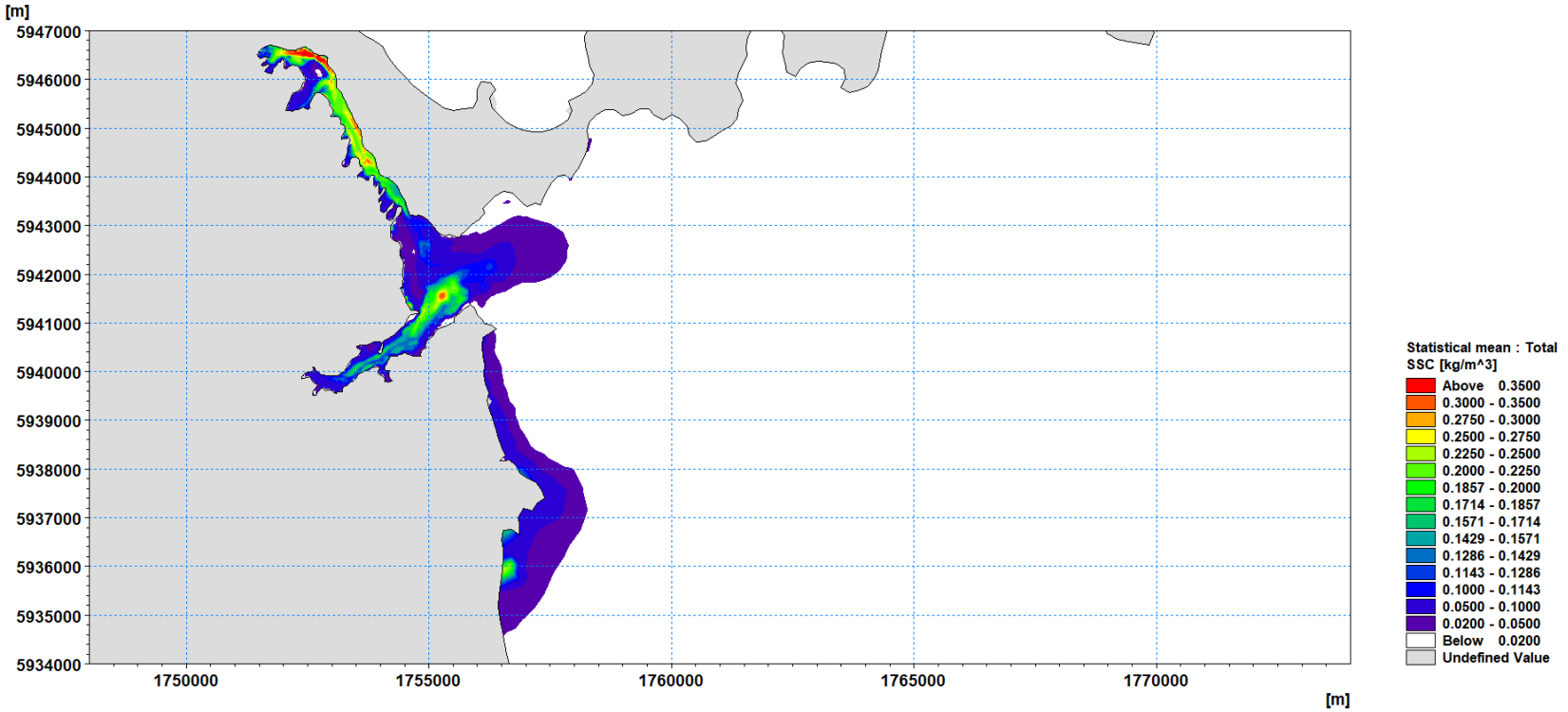

Figure 6-6. Mean total suspended sediment concentration in the top layer of the model over the duration of the May event.

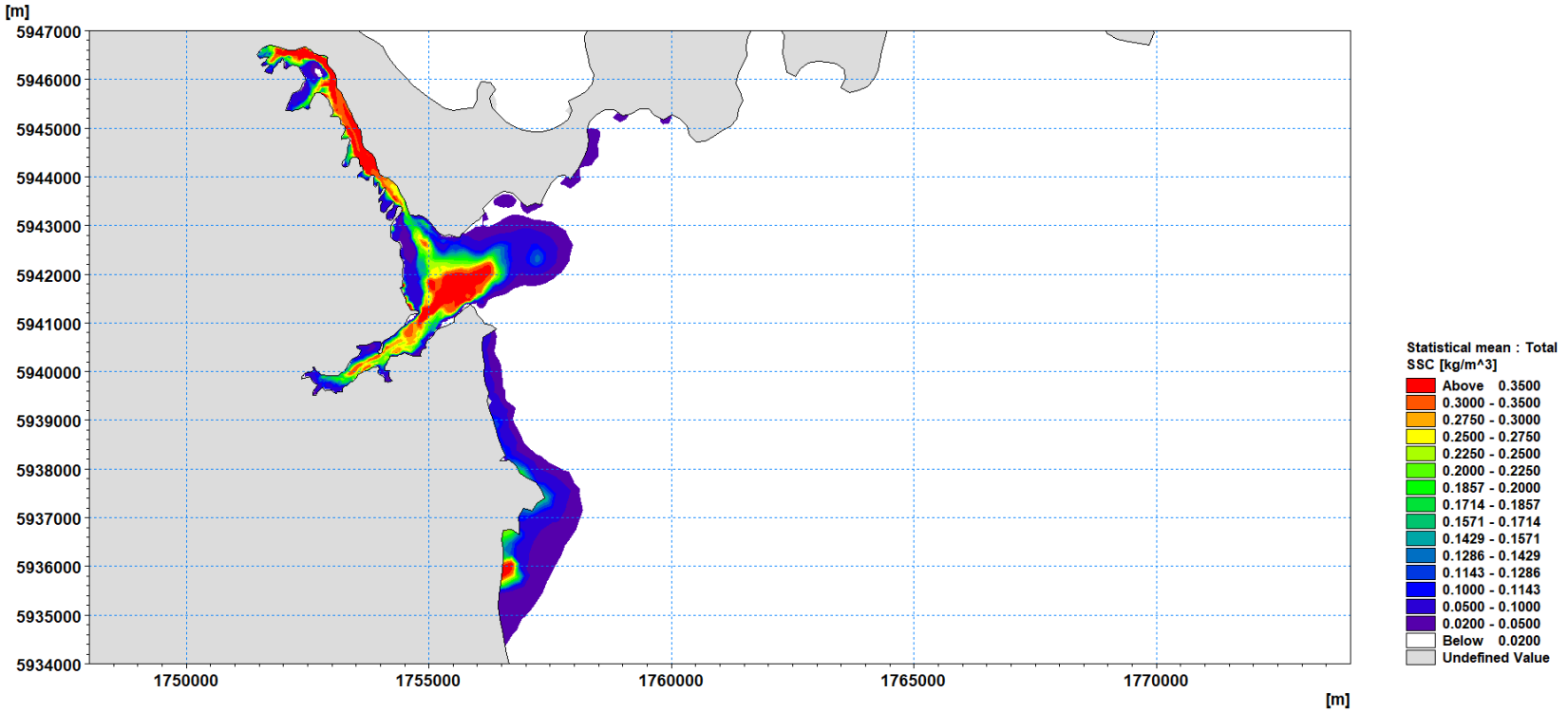

Figure 6-7. Mean total suspended sediment concentration in middle of the water column over the duration of the May event.

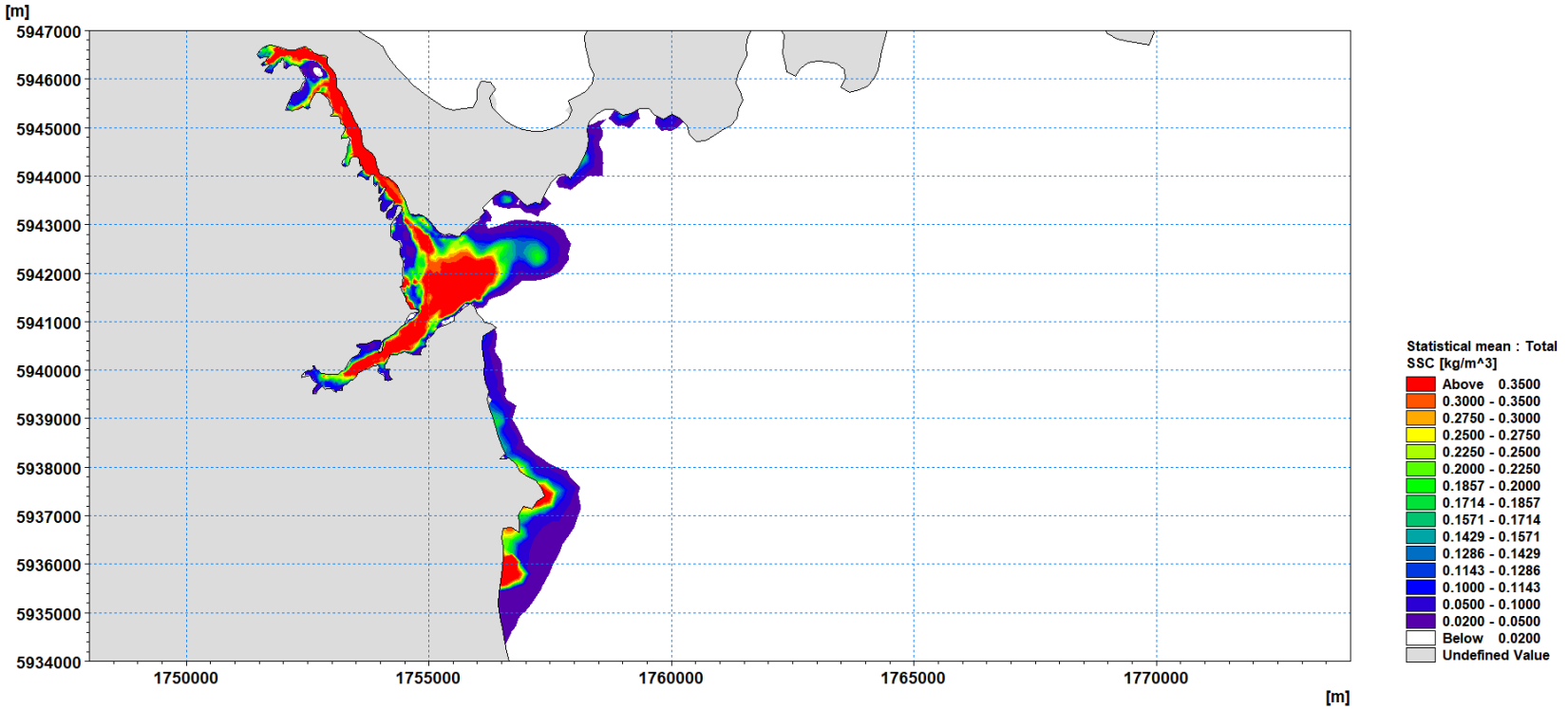

Figure 6-8. Mean near-bed total suspended sediment concentration over the duration of the May event.

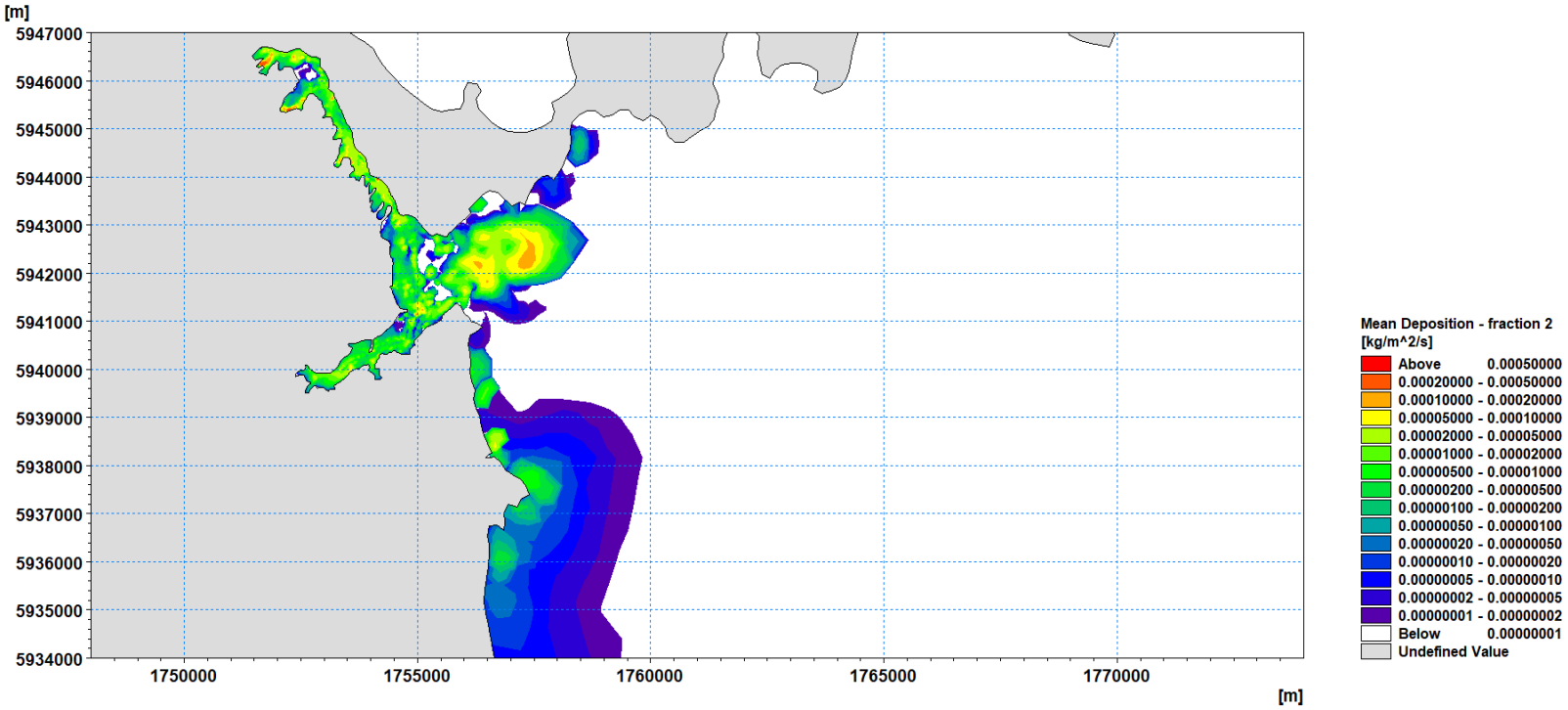

Figure 6-9. Spatial pattern of mean deposition rate over the duration of the May event.

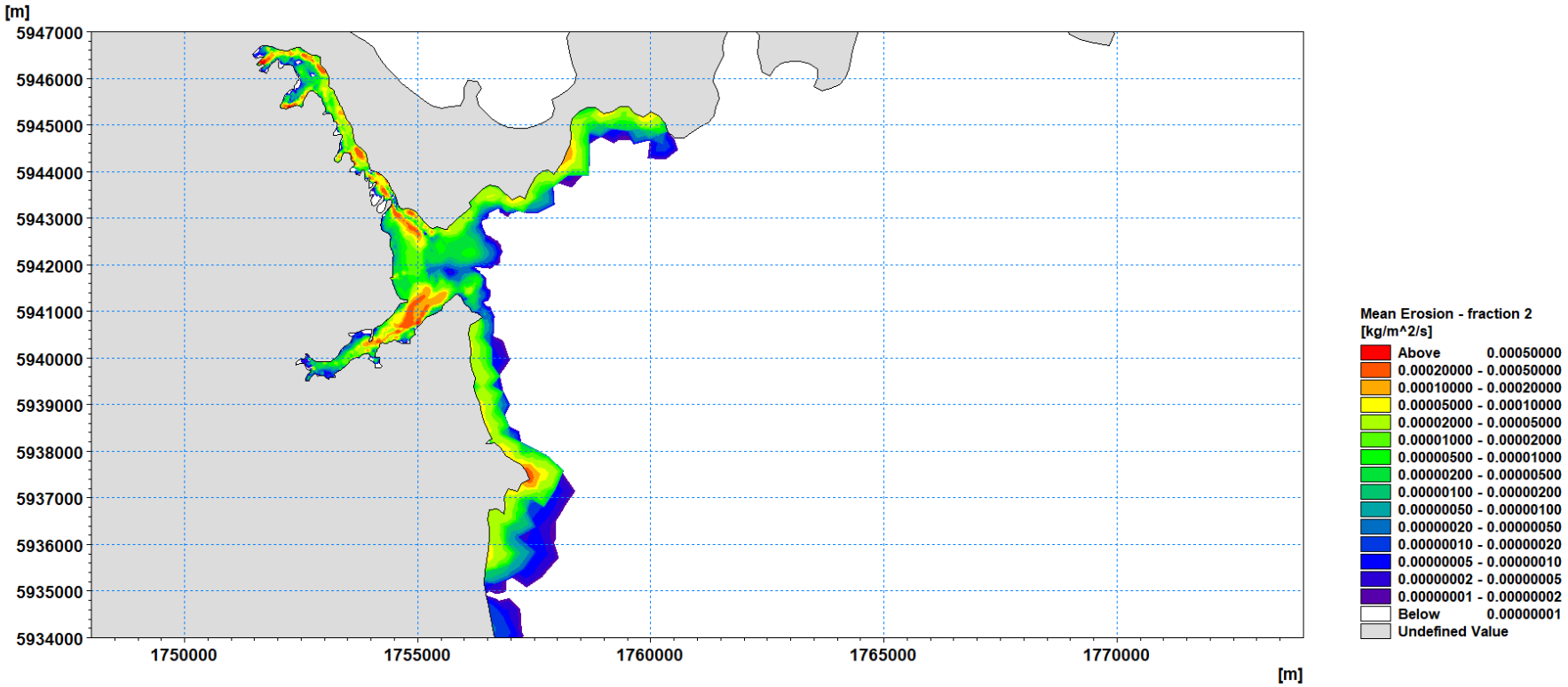

Figure 6-10. Spatial pattern of mean erosion rate over the duration of the May event.

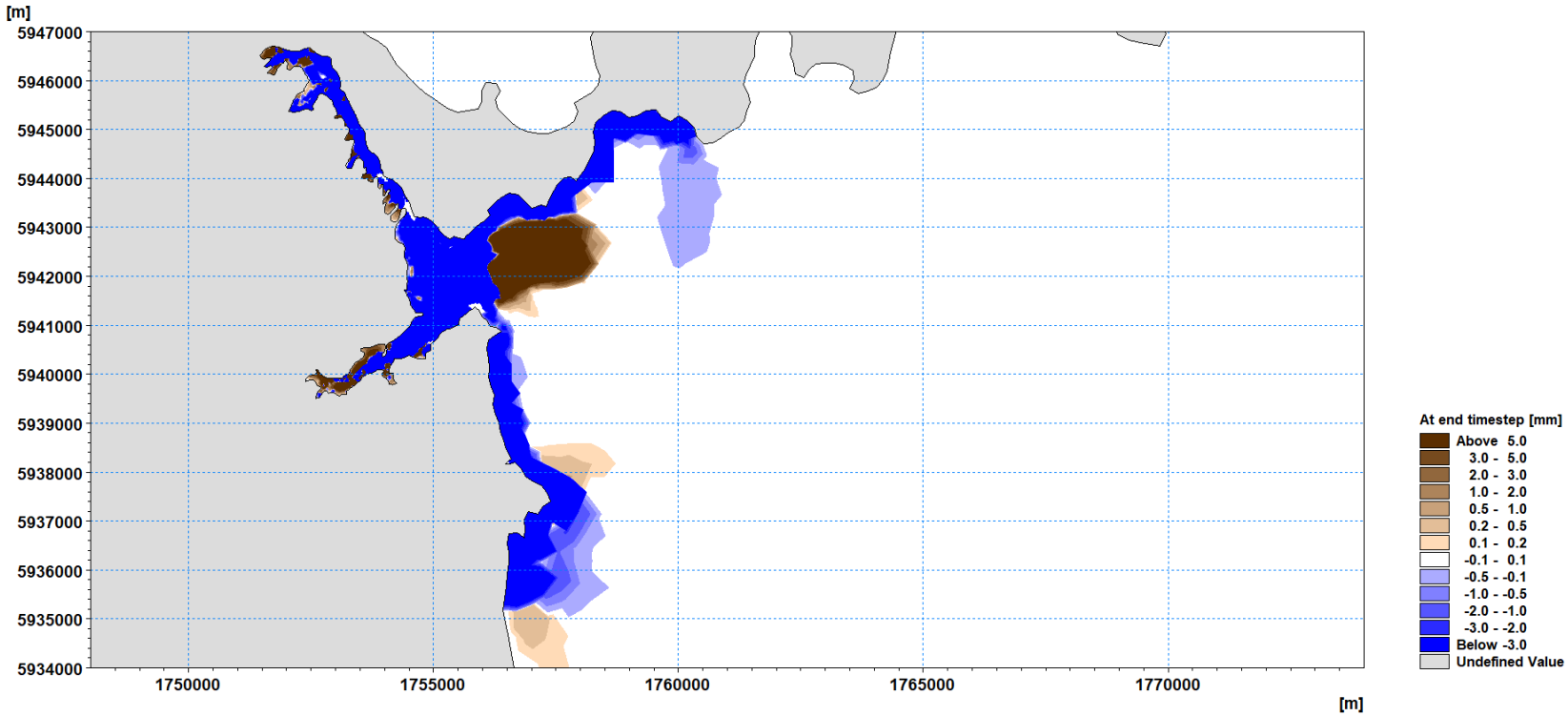

Figure 6-11. Change in bed level (mm) at the end of the May event simulation.

References

DHI, 2018. Okura Weiti Sediment Transport Modelling - Data report 44801163/01 prepared for Auckland Council.

DHI, 2017a. MIKE 21 Flow Model FM, Hydrodynamic Module, User Guide.

DHI, 2017b. MIKE 21 SW, Spectral Wave FM Module, User Guide.

DHI, 2017c. MIKE 3 Flow Model FM, Mud Transport Module, User Guide.

DHI, 2017d. MIKE C-MAP, Extraction of World Wide Bathymetry Data and Tidal Information, User Guide.

Greig, M.J., 1990. Circulation in the hauraki Gulf, New Zealand. N. Z. J. Mar. Freshw. Res. 24, 141–150.

Partheniades, E., 1965. Erosion and deposition of cohesive soils. J. Hydraul. Div. 91, 105–139.

Pritchard, M., Reeve, G., Swales, S. 2009. Modelling storm-load sediment deposition thresholds for potential ecological effects in Okura Estuary / Karepiro Bay: Model development and calibration. NIWA Client Report No. HAM2009–106.

Appendix A. FWMT Linkages

Linkages between the FWMT catchment outlets on the marine receiving environment inputs.

MIKE 3 Catchment Outlet Sites	FWMT node numbers
North Outlet	100823, 100284
Awaruku	100291, 100292
Long Bay	100285, 100286, 100290
SS Outer	100282
SS Mid-East	100279, 100280
SS Mid-West	100278
SS Inner	100277
Redvale	100260, 100270, 100274, 100275, 100276
North Arm	100251, 100252, 100257, 10058
North Shore	100250
Karepiro	100244, 100249
Karepiro Beach	100245
Stillwater	100240, 100241, 100242, 100243
Weiti South	100233
Silverdale	100205, 100206, 100225, 100226, 100227, 100228, 100230, 100231, 100232
Arkle Bay	100201, 100202
Whangaparaoa	100204*
Weiti North	100204*
Duck Creek	100239

* River flows at the Whangaparaoa and Weiti North locations in MIKE 3 were extracted from Site 100204 applying 50% of the original river flow.